universe

IMPACT FACTOR 2.5

CITESCORE 4.3

Article

Universal Properties of the Evolution of the Universe in Modified Loop Quantum Cosmology

Jamal Saeed, Rui Pan, Christian Brown, Gerald Cleaver and Anzhong Wang

Special Issue

Loop Quantum Gravity and Non-Perturbative Approaches to Quantum Cosmology, Second Edition

Edited by

Prof. Dr. Gerald B. Cleaver

MDPI

https://doi.org/10.3390/universe10100397

universe

MDPI

Article

Universal Properties of the Evolution of the Universe in Modified Loop Quantum Cosmology

Jamal Saeed [1], Rui Pan [1], Christian Brown [2], Gerald Cleaver [2] and Anzhong Wang [1,*]

[1] GCAP-CASPER, Physics Department, Baylor University, Waco, TX 76798-7316, USA; jamal_saeed1@baylor.edu (J.S.); rui_pan1@baylor.edu (R.P.)
[2] EUCOS-CASPER, Physics Department, Baylor University, Waco, TX 76798-7316, USA; christian_brown4@baylor.edu (C.B.); gerald_cleaver@baylor.edu (G.C.)
* Correspondence: anzhong_wang@baylor.edu

Abstract: In this paper, we systematically study the evolution of the Universe within the framework of a modified loop quantum cosmological model (mLQC-I) using various inflationary potentials, including chaotic, Starobinsky, generalized Starobinsky, polynomials of the first and second kinds, generalized T-models and natural inflation. In all these models, the big bang singularity is replaced by a quantum bounce, and the evolution of the Universe, both before and after the bounce, is *universal and weakly dependent on the inflationary potentials*, as long as the evolution is dominated by the kinetic energy of the inflaton at the bounce. In particular, the pre-bounce evolution can be *universally* divided into three different phases: *pre-bouncing, pre-transition, and pre-de Sitter*. The pre-bouncing phase occurs immediately before the quantum bounce, during which the evolution of the Universe is dominated by the kinetic energy of the inflaton. Thus, the equation of state of the inflaton is about one, $w(\phi) \simeq 1$. Soon, the inflation potential takes over, so $w(\phi)$ rapidly falls from one to negative one. This pre-transition phase is very short and quickly turns into the pre-de Sitter phase, whereby the effective cosmological constant of Planck size takes over and dominates the rest of the contracting phase. Throughout the entire pre-bounce regime, the evolution of both the expansion factor and the inflaton can be approximated by universal analytical solutions, independent of the specific inflation potentials.

Keywords: quantum gravity; quantum cosmology; quantum bounce; evolution of universe

Citation: Saeed, J.; Pan, R.; Brown, C.; Cleaver, G.; Wang, A. Universal Properties of the Evolution of the Universe in Modified Loop Quantum Cosmology. *Universe* **2024**, *10*, 397. https://doi.org/10.3390/universe10100397

Received: 20 August 2024
Revised: 10 October 2024
Accepted: 12 October 2024
Published: 15 October 2024

1. Introduction

Since its inception in 1980 [1], the inflationary paradigm has achieved great success, resolving many long-standing problems of the standard big bang cosmology. This paradigm has remained consistent with all cosmological and astrophysical observations conducted to date [2]. However, inflation remains past-incomplete [3], due to the Big Bang singularity, where all physical quantities become infinite. Hence, the initial conditions of inflation are usually imposed at a moment sufficiently far from the singularity but early enough so that the wavelengths of all the observational modes are within the Hubble horizon.

A natural question then arises: What happened before inflation? This important question is expected to be answered by quantum gravity (QG), a theory that has not yet been established, despite enormous efforts in the past century. Several candidates have been proposed, including string/M-theory [4,5] and loop quantum gravity (LQG) [6–10]. In particular, in the last two decades, LQG has been rigorously applied to understand singularity resolution in various cosmological models (for reviews, see Refs. [11–19]). In all these models, a coherent picture of Planck-scale physics has emerged: *the big bang singularity is replaced by a quantum bounce*[1]. This framework is often referred to as loop quantum cosmology (LQC).

The physical implications of LQC have also been studied using *the effective descriptions* of the quantum spacetime derived from coherent states [32], whose validity has been

verified for various spacetimes numerically [33,34], especially for states that sharply peaked on classical trajectories at late times [35]. Effective dynamics provide a definitive answer to the resolution of the big bang singularity, replaced by a quantum bounce when the energy density of matter reaches a maximum value determined purely by the underlying quantum geometry [12,16,18,19].

Despite extensive results on singularity resolution and phenomenology of the very early universe obtained in the framework of LQC, an important issue that has remained open is its connection to LQG (see, for example, ref. [36,37] for discussions). The starting point of LQC is to first classically reduce the Hamiltonian from infinitely many to a few gravitational degrees of freedom by imposing homogeneity and then to quantize the classically reduced Hamiltonian using the techniques of LQG. However, in LQG, the processes of symmetry reduction and quantization do not commute in general, and it is important to understand how well the physics of the full LQG is captured by LQC. In addition, in LQG, the Hamiltonian usually consists of two parts, the Euclidean and Lorentz parts, and one follows different processes to quantize each part [6–10]. However, in LQC, only the quantization of the Euclidean part was considered by taking advantage of the properties of the classical Hamiltonian, in which the Euclidean and Lorentz parts are proportional to each other for the flat Friedmann–Lemaítre–Robertson–Walker (FLRW) universe [12].

Over the past decade, the above issue has been extensively studied using both bottom-up and top-down approaches, from which an important conclusion is emerging: *LQC and its major predictions are robust*. In particular, the Big Bang singularity is resolved in the models studied so far. However, dramatic changes in the evolution of the universe in the pre-bounce phase are also found [38].

In the bottom-up approach [39], symmetries are still imposed before quantization, but the Lorentzian term is treated independently by applying Thiemann's regularization from the full theory of LQG [40,41]. In doing so, it was found that the resultant wave function is now described by a fourth-order difference Equation [39], which is referred to as mLQC-I [38]. For a systematic derivation of the model, we refer readers to [42,43]. For sharply peaked states, the resulting quantum dynamics are well described by effective Friedman–Raychaudhuri (FR) Equations [44], with which it was found that both the resolution of the big bang singularity [45] and the existence of a subsequent desired slow-roll inflation are generic [46].

In the top-down approach, using complexifier coherent states and treating the Euclidean and Lorentzian terms in the scalar constraint separately as in full LQG, Dapor and Liegener (DL) first obtained a modified LQC model [47,48], which is quite similar to mLQC-I but with the μ_0-scheme, as DL used a fixed graph [47,48]. To address this shortcoming, the DL work was extended to allow for graph-changing dynamics in an approach based on the path-integral reformulation of LQG [49], whereby a consistent mLQC-I model can be obtained.

In this paper, we shall systematically study the evolution of the Universe within the framework of mLQC-I. Note that such studies have already been conducted in the post-bounce regime ($t \geq t_B$) in [38,44–46,50–53], where t_B denotes the bounce time. It was found that the evolution in this regime is universal and independent of the inflationary potential, as long as the evolution is dominated at the quantum bounce by the kinetic energy of the inflation

$$\frac{1}{2}\dot{\phi}_B^2 \gg V(\phi_B), \tag{1}$$

where an over dot denotes the derivative with respect to the cosmic time, and ϕ_B is the value of the inflation at the bounce. Initial conditions satisfying Equation (1) are important because they always lead to slow-roll inflation [38,44–46], quick similar to that in LQC [54–61]. Therefore, in this paper, we focus on the pre-bounce regime ($t \leq t_B$), which has not been studied adequately so far and is important, especially when the initial conditions of cosmological perturbations are imposed in the contracting phase [12,16,18,19].

Specifically, the rest of the paper is organized as follows: In Section 2, we briefly review the mLQC-I model and write down the dynamical Hamiltonian equations. To understand the major properties of mLQC-I, we also provide the corresponding FR equations. In Section 3, we study the evolution of the Universe with several inflationary potentials, including chaotic, Starobinsky, generalized Starobinsky, polynomials of the first and second kinds, generalized T-models, and natural inflation. In the last case, we consider several choices of parameters involved in the model. Note that the chaotic and natural inflationary models have some tensions with current observations [2]. The reasons that we still consider them here are two-fold: First, after quantum gravitational effects are taken into account, such tensions can be alleviated [62]. Second, the universal properties of the evolution of the universe, both before and after the quantum bounce, are independent of the choice of inflationary potentials in LQC [55–61,63]. We find that this is also true in mLQC-I. In all these models, we find that the evolution of the Universe in the pre-bounce regime ($t \leq t_B$) is universal and weakly depends on the inflationary potentials, as long as the kinetic-energy-dominated condition (1) is satisfied at the bounce. In all these models, the evolution is clearly divided into three different epochs, *pre-bouncing, pre-transition, and pre-de Sitter*, as defined by Equation (35), in terms of the equation of state of the inflation

$$w(\phi) \equiv \frac{P(\phi)}{\rho(\phi)}, \tag{2}$$

where $P(\phi)$ and $\rho(\phi)$ are the pressure and energy density of the inflationary field, respectively, given by Equation (6). Physically, it can be understood as follows: In the pre-bouncing phase, the evolution of the universe is dominated by the kinetic energy as determined by the initial conditions imposed at the bounce, so it is expected that its evolution in this phase is independent of the inflationary potentials and $w(\phi) \simeq +1$. However, an effective Planck-size cosmological constant exists in the pre-bounce regime [cf. Equation (21)], so it will soon dominate the evolution once apart from the bounce, during which we have $w(\phi) \simeq -1$. Clearly, during this phase the evolution of the universe will be also independent of the inflationary potentials. In between these two phases, a short pre-transition phase exists, during which $w(\phi)$ drops rapidly from $+1$ to -1 and behaves like a step function[2] As a result, in these epochs the expansion factor $a(t)$ and the inflaton $\phi(t)$ are universal, as shown explicitly by Figure 28 of Section 4. In this Section, we also show that $a(t)$ and $\phi(t)$ can be well-approximated by Equations (45) and (48), respectively, where d_n and e_n are constants determined by fitting the analytical expressions with their numerical solutions, as given in Section 4. Therefore, *the evolution of the Universe in both the pre-bounce regime ($t \leq t_B$) and the post-bounce regime ($t \geq t_B$) is universal in mLQC-I* [38,44–46]. This is important and will significantly facilitate the studies of cosmological perturbations [16,64–67], as already shown in LQC [56]. The paper ends in Section 5, in which our main results and concluding remarks are presented.

2. Effective Dynamics of Modified Loop Quantum Cosmology

In this section, we provide a summary of the modified Friedmann dynamics for mLQC-I [38]. Its dynamics can be obtained directly from the effective Hamiltonian, given by [39]

$$\mathcal{H} = \frac{3v}{8\pi G\lambda^2}\left\{\sin^2(\lambda b) - \frac{(\gamma^2+1)\sin^2(2\lambda b)}{4\gamma^2}\right\} + \mathcal{H}_{\mathcal{M}}, \tag{3}$$

where G is the Newtonian constant, $v \equiv v_0 a^3$, and v_0 is the volume of a fiducial cell in the $\mathcal{R}^3$ spatial manifold, and a is the expansion factor of the Universe. The variable b denotes the momentum conjugate of v and satisfies the canonical relation

$$\{b, v\} = 4\pi G\gamma, \tag{4}$$

where γ is known as the Barbero–Immirzi parameter whose value is set to $\gamma \approx 0.2375$ using black hole thermodynamics in LQG [68]. The parameter λ is defined as $\lambda^2 \equiv \Delta = 4\sqrt{3}\pi\gamma\ell_{Pl}^2$, where Δ denotes the minimal area gap of the area operator in LQG [7,12,69,70].

In this paper, we consider only the case in which the matter is characterized by a single scalar field ϕ with potential $V(\phi)$, for which $\mathcal{H}_M$ is given by

$$\mathcal{H}_M = \frac{1}{2}v\left(\frac{p_\phi^2}{v^2} + 2V(\phi)\right), \tag{5}$$

where p_ϕ is the momentum of ϕ. Then, the corresponding energy density and pressure of the scalar field are given by

$$\begin{aligned} \rho &\equiv \tfrac{\mathcal{H}_M}{v} = \tfrac{1}{2}\dot{\phi}^2 + V(\phi), \\ P &\equiv -\tfrac{\partial \mathcal{H}_M}{\partial v} = \tfrac{1}{2}\dot{\phi}^2 - V(\phi). \end{aligned} \tag{6}$$

The basic variables b, v, ϕ and p_ϕ satisfy the Hamiltonian equations

$$\begin{aligned} \dot{v}s. &= \{v, \mathcal{H}\} \\ &= \tfrac{3v\sin(2\lambda b)}{2\gamma\lambda}\left\{(\gamma^2+1)\cos(2\lambda b) - \gamma^2\right\}, \end{aligned} \tag{7}$$

$$\begin{aligned} \dot{b} &= \{b, \mathcal{H}\} = \tfrac{3\sin^2(\lambda b)}{2\gamma\lambda^2}\left\{\gamma^2\sin^2(\lambda b) - \cos^2(\lambda b)\right\} \\ &\quad - 4\pi G\gamma P, \end{aligned} \tag{8}$$

$$\dot{\phi} = \{\phi, \mathcal{H}\} = \frac{p_\phi}{v}, \tag{9}$$

$$\dot{p}_\phi = \{p_\phi, \mathcal{H}\} = -vs.V_{,\phi}, \tag{10}$$

where $V_{,\phi} \equiv dV(\phi)/d\phi$. Equations (7)–(10) are the first-order ordinary differential equations for the four canonical variables $(v, b; \phi, p_\phi)$. Once the initial conditions are specified at a given moment, for example, $t = t_B$, they uniquely determine the trajectory of the evolution of the Universe. Such initial conditions are often imposed at the quantum bounce [12,38], at which the expansion factor reaches its minimal value and the energy density reaches its maximum.

To see the above clearly, it is instructive to recast the above four dynamical equations in the form of the modified FR Equations [38]

$$H^2 = \frac{8\pi G\rho}{3}\left(1 - \frac{\rho}{\rho_c^{\mathrm{I}}}\right)\left(1 + \frac{\gamma^2\rho/\rho_c^{\mathrm{I}}}{(\gamma^2+1)\left(1+\sqrt{1-\rho/\rho_c^{\mathrm{I}}}\right)^2}\right), \quad (t \geq t_B), \tag{11}$$

$$\begin{aligned} \tfrac{\ddot{a}}{a} &= -\tfrac{4\pi G}{3}(\rho + 3P) + \tfrac{4\pi G\rho^2}{3\rho_c^{\mathrm{I}}}\left(\tfrac{\left(7\gamma^2+8\right) - 4\rho/\rho_c^{\mathrm{I}}\left(5\gamma^2+8\right)\sqrt{1-\rho/\rho_c^{\mathrm{I}}}}{(\gamma^2+1)\left(1+\sqrt{1-\rho/\rho_c^{\mathrm{I}}}\right)^2}\right) \\ &\quad + 4\pi GP\left(\tfrac{3\gamma^2+2+2\sqrt{1-\rho/\rho_c^{\mathrm{I}}}}{(\gamma^2+1)\left(1+\sqrt{1-\rho/\rho_c^{\mathrm{I}}}\right)}\right)\tfrac{\rho}{\rho_c^{\mathrm{I}}}, \quad (t \geq t_B), \end{aligned} \tag{12}$$

where $H \equiv \dot{v}/(3v) = \dot{a}/a$, and

$$\rho_c^{\mathrm{I}} \equiv \frac{\rho_c}{4(1+\gamma^2)}, \quad \rho_c \equiv \frac{3}{8\pi\lambda^2\gamma^2 G}. \tag{13}$$

It is evident from these two equations that the energy conservation law $\dot{\rho} + 3H(\rho + P) = 0$ holds. Substituting Equation (6) into this equation, we find

$$\ddot{\phi} + 3H\dot{\phi} + V_{,\phi} = 0, \tag{14}$$

while in terms of ρ and P, we also have

$$\dot{b} = -4\pi G\gamma(\rho + P) = -4\pi G\gamma\dot{\phi}^2. \tag{15}$$

It should be noted that, Equations (11) and (12) hold only after the quantum bounce ($t \geq t_B$), as already indicated in these equations, at which we have $\rho(t_B) = \rho_c^{\rm I}$ and $H(t_B) = 0$, so the expansion factor reaches its minimal value $a_B \equiv a(t_B)$. When $t \gg t_B$ (or equivalently, $\rho/\rho_c^{\rm I} \ll 1$), Equations (11) and (12) reduce to their relativistic limits

$$H^2 \simeq \frac{8\pi G}{3}\rho, \ (t \gg t_B), \tag{16}$$

$$\frac{\ddot{a}}{a} \simeq -\frac{4\pi G}{3}(\rho + 3P), \ (t \gg t_B). \tag{17}$$

In particular, it is interesting to note that $\rho/\rho_c^{\rm I} \simeq 10^{-12}$ at the onset of inflation [12,38]. Therefore, during the inflationary phase, the modified FR equations are well approximated by their classical limits (16) and (17).

In the pre-bounce phase ($t \leq t_B$), the modified FR equations take the form [38]

$$H^2 = \frac{8\pi G_\alpha \rho_\Lambda}{3}\left(1 - \frac{\rho}{\rho_c^{\rm I}}\right)\left(1 + \frac{\rho\left(1 - 2\gamma^2 + \sqrt{1 - \rho/\rho_c^{\rm I}}\right)}{4\gamma^2\rho_c^{\rm I}\left(1 + \sqrt{1 - \rho/\rho_c^{\rm I}}\right)}\right), \quad (t \leq t_B), \tag{18}$$

$$\begin{aligned}\frac{\ddot{a}}{a} = &-\tfrac{4\pi G_\alpha}{3}(\rho + 3P - 2\rho_\Lambda) + 4\pi G_\alpha P\left(\frac{2 - 3\gamma^2 + 2\sqrt{1 - \rho/\rho_c^{\rm I}}}{(1 - 5\gamma^2)\left(1 + \sqrt{1 - \rho/\rho_c^{\rm I}}\right)}\right)\frac{\rho}{\rho_c^{\rm I}} \\ &- \frac{4\pi G_\alpha \rho^2\left(2\gamma^2 + 5\gamma^2\left(1 + \sqrt{1 - \rho/\rho_c^{\rm I}}\right) - 4\left(1 + \sqrt{1 - \rho/\rho_c^{\rm I}}\right)^2\right)}{3\rho_c^{\rm I}(1 - 5\gamma^2)\left(1 + \sqrt{1 - \rho/\rho_c^{\rm I}}\right)^2}, \quad (t \leq t_B),\end{aligned} \tag{19}$$

where $G_\alpha \equiv \alpha G$, and

$$\alpha \equiv \frac{1 - 5\gamma^2}{\gamma^2 + 1}, \quad \rho_\Lambda \equiv \frac{3}{8\pi G\alpha\lambda^2(1 + \gamma^2)^2}. \tag{20}$$

From Equations (18) and (19), we can see that at the bounce $\rho(t_B) = \rho_c^{\rm I}$, the universe contracts to its minimal volume $v = v_0 a_B^3$ at $t = t_B$. Afterward, it smoothly passes to the expansion phase, but is now described by Equations (11) and (12). The smoothness is shown explicitly in [44–46], and can be also seen from Equations (14) and (15), which hold across the bounce.

When $t \ll t_B$ (or $\rho/\rho_c^{\rm I} \ll 1$), Equations (18) and (19) reduce to

$$H^2 \simeq \frac{8\pi G_\alpha}{3}\rho_\Lambda\left(1 - \frac{\rho}{\rho_\Lambda}\right), \ (t \ll t_B), \tag{21}$$

$$\frac{\ddot{a}}{a} \simeq \frac{8\pi G_\alpha}{3}\rho_\Lambda\left(1 - \frac{\rho + 3P}{2\rho_\Lambda}\right), \ (t \ll t_B), \tag{22}$$

which are quite different from Equations (16) and (17). In particular, the effective Planck-scale cosmological constant ρ_Λ soon dominates the evolution of the pre-bounce phase, whereby a de Sitter spacetime is obtained in the pre-bounce phase but with a Planck-scale cosmological constant $\rho_\Lambda \simeq \mathcal{O}(\rho_{\rm pl})$. In addition, the Newtonian constant G is replaced by $G_\alpha (= \alpha G)$, where α is defined by Equation (20). More remarkably, this Planck-scale cosmological constant is filtered out by the quantum bounce and disappears miraculously after the bounce, whereby the classical FR equations are obtained, as shown explicitly by

Equations (16) and (17). This is significantly different from LQC [12], in which the evolution of the Universe is symmetric with respect to the bounce[3].

The background evolution of the universe in the post-bounce regime ($t \geq t_B$) has been studied extensively in [38,44–46], with various potentials, including chaotic, fractional monodromy, Starobinsky, and non-minimally coupling Higgs potentials. Among several remarkable features, it was found that *the evolution of the universe is universal for any given potential, as long as the initial conditions imposed at the bounce are kinetic-energy-dominated*, that is

$$\frac{1}{2}\dot{\phi}_B^2 \gg V(\phi_B), \tag{23}$$

where $\phi_B (\equiv \phi(t_B))$ is the value of the scalar field at the bounce. Moreover, evolution can be universally divided into three phases:

$$\begin{aligned} &(i)\ \text{bouncing}\ (w(t) \simeq 1), \\ &(ii)\ \text{transition}\ (-1 < w(t) < 1), \\ &(iii)\ \text{inflationary},\ (w(t) \simeq -1), \end{aligned} \tag{24}$$

as shown in Figure 1. Here, the equation of state of the scalar field $w(t)$ is defined as follows:

$$w(t) \equiv \frac{P(t)}{\rho(t)} = \frac{\frac{1}{2}\dot{\phi}^2 - V}{\frac{1}{2}\dot{\phi}^2 + V}. \tag{25}$$

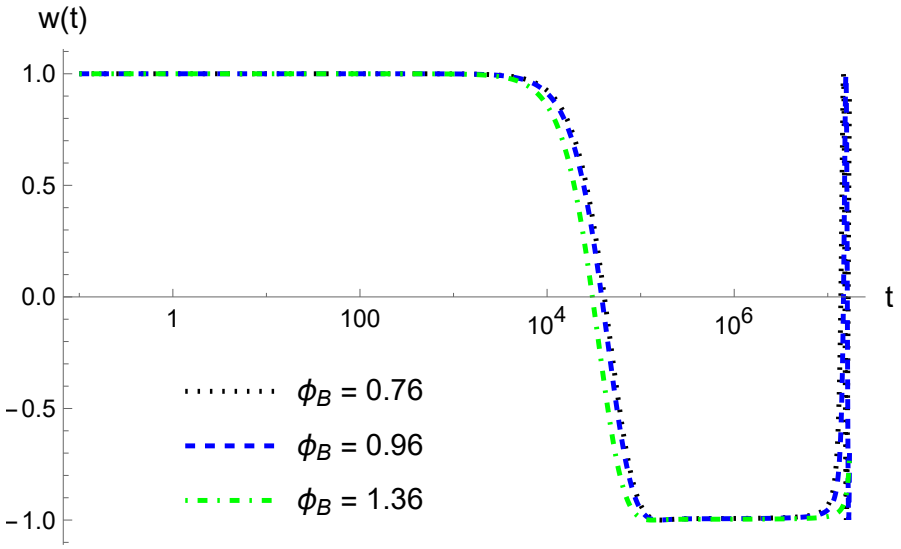

Figure 1. The evolution $w(t)$ of the equation of state in the post-bounce phase ($t \geq t_B$) for the chaotic potential with different initial conditions ϕ_B for $\dot{\phi}_B > 0$. In this plot, t_B is set to zero. It should be noted that the equation of state, $w(t)$, behaves the same not only for $\dot{\phi}_B < 0$ with the same chaotic potential, but also for other potentials, as long as the evolution of the universe at the bounce is kinetic-energy dominated [38,44–46].

It should be noted that in Figure 1, only the case of the chaotic potential was considered. However, the general behavior of the evolution of the universe is universal and independent of the choice of potential, as long as the initial conditions are kinetic-energy dominated. These remarkable features are also shared by LQC, first found in [56] and later confirmed in various studies [57–61].

Moreover, during the bouncing phase, the expansion factor $a(t)$ and the scalar field $\phi(t)$ can be well described by the analytical solution [46]

$$\begin{aligned} a(t) &= \left(1+24\pi\rho_c^I\left(1+\tfrac{A_0\gamma}{1+B_0 t}\right)t^2\right)^{\frac{1}{6}}, \\ \phi(t) &= \phi_B+\mathrm{sgn}(\dot\phi_B)\frac{\sinh^{-1}\sqrt{24\pi\rho_c^I\left(1+\frac{C_0\gamma^2}{1+D_0 t}\right)t}}{\sqrt{12\pi\left(1+\frac{C_0\gamma^2}{1+D_0 t}\right)}}, \end{aligned} \tag{26}$$

where $A_0 = 1.2$, $B_0 = 6$, $C_0 = 1.2$, and $D_0 = 2$ with relative errors no larger than 0.3%, as shown in Figure 2. Again, the analytical solutions are universal and independent of the choice of inflationary potential $V(\phi)$ as long as the initial kinetic-energy dominated condition (1) holds.

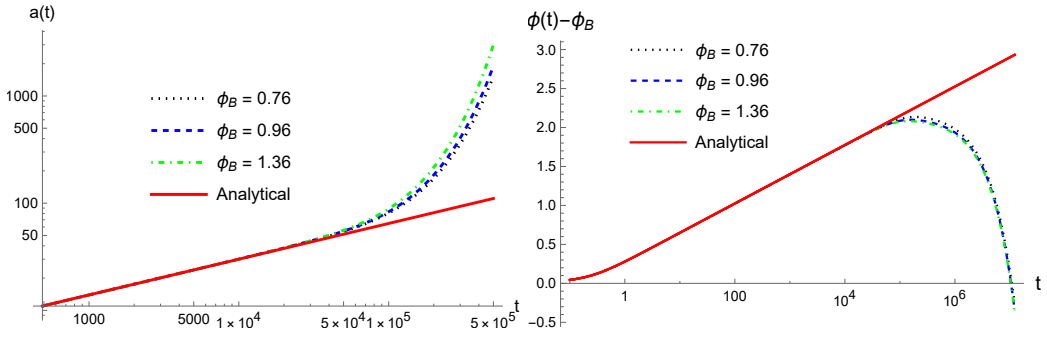

Figure 2. The numerical and analytical solutions of $a(t)$ and $\phi(t)$ for different initial values of ϕ_B that result in at least 50 e-folds for the chaotic potential with $\dot\phi_B > 0$. This universal behavior is true for any given inflation potential $V(\phi)$ as long as the condition (23) holds at the bounce.

In addition, it was shown that the probability of the occurrence of a desired slow-roll inflation is generic. In particular, it was found that for such a desired slow-roll inflation to not occur, the probability is [46]

$$P_{\text{mLQC-I}}(\text{not realized}) \lesssim 1.12\times 10^{-5}, \tag{27}$$

where "desired" means the one that is consistent with current observations. This is comparable to $P_{\text{LQC}}(\text{not realized}) \lesssim 2.74\times 10^{-6}$, obtained in LQC [71,72].

Therefore, in this paper, we shall focus on the evolution of the universe in the pre-bounce regime ($t \le t_B$) and pay particular attention to the universal properties of evolution.

3. Numerical Solutions of the Evolution of the Universe

Since the kinetic-energy-dominated initial conditions imposed at the bounce always lead to slow-roll inflation for any given potential, in the rest of this paper, we shall consider only such initial conditions with several well-studied inflationary potentials [2,73], including *chaotic, Starobinsky, α-attractive, and natural inflation potentials*.

The advantage of imposing the initial conditions at the bounce is that $\dot\phi_B$ is determined uniquely up to a sign for any given initial data ϕ_B via the relation $\rho(t_B) = \rho_c^{\text{I}}$, which yields

$$\dot\phi_B = \pm\sqrt{2(\rho_c^{\text{I}} - V(\phi_B))}. \tag{28}$$

On the other hand, from Equations (11), (12), (18) and (19), we can see that these equations are scaling-invariant with respect to the expansion factor $a \to a/L_o$. Therefore, without loss of generality, we can always set $a_B = 1$. Then, the initial conditions are reduced to the choice of

$$(\phi_B, \mathrm{sgn}(\dot\phi_B)). \tag{29}$$

In addition, using the translation invariance $t \to t + t_0$, in the rest of this paper, we shall set $t_B = 0$.

To process further, following [38,45,46,74], let us first introduce the following physical quantities:

- The first-order Hubble rate and potential slow-roll parameters

$$\epsilon_H = -\frac{\dot{H}}{H^2}, \qquad \eta_H = -\frac{\ddot{H}}{2H\dot{H}}, \tag{30a}$$

$$\epsilon_V = \frac{1}{16\pi G}\left(\frac{V_{,\phi}}{V}\right)^2, \qquad \eta_V = \frac{V_{,\phi\phi}}{8\pi G V}. \tag{30b}$$

These sets of slow-roll parameters are typically used for different purposes [75]. In particular, the slow-roll parameters with the subscript "V" can be used to determine which part of the potential can successfully drive inflation. On the other hand, slow-roll parameters with subscript "H" are used for numerical simulations to define when slow-roll inflation begins and ends. In the classical regime, the scale factor acceleration equation satisfies the following relation:

$$\ddot{a} = aH^2(1 - \epsilon_H). \tag{31}$$

The Universe experiences an accelerated expansion when $\epsilon_H < 1$, whereas slow-roll inflation occurs only when $\epsilon_H \ll 1$ and $\eta_H \ll 1$ [75]. For the sake of concreteness, we define the onset of inflation as the time t_i when $|\eta_H| = 0.03$ for the first time in the transition phase. The end of the slow-roll inflation is defined at the time $t_{\rm end}$ when $|\epsilon_H| = 1$ for the first time after t_i.

- The e-fold N during the inflationary phase: This number is usually defined as follows:

$$N = \ln\left(\frac{a(t_{\rm end})}{a(t_i)}\right). \tag{32}$$

To have a successful slow-roll inflation, the inflation potential has to be very flat, so that the Universe can expand large enough [75]. All the cosmological problems can be resolved if the Universe expands about 60 e-fold during the inflationary phase, although its exact value depends on the inflationary models [2]. Therefore, in the following one will see that the minimal e-fold $N_{\rm min}$ will be different in different models.

With the above in mind, we are now ready to solve the four dynamical Equations (7)–(10) for any given initial conditions (29)[4]. In the following, we shall study the chaotic, Staribinsky, α-attractor, and natural inflation potentials, separately.

3.1. Chaotic Potential

The chaotic inflationary potential is given by [76]

$$V(\phi) = \frac{1}{2}m^2\phi^2, \tag{33}$$

where the mass is set to $m = 1.26 \times 10^{-6}\, m_{pl}$ [2]. Since it has already been shown that the occurrence of a desired slow-roll inflation is generic [46], it is sufficient for us to find the initial conditions that lead to $N \geq 45$ e-folds.

In this model, the modified Friedmann and Klein–Gordon equations are invariant under the replacement

$$(\phi, \dot{\phi}) \to (-\phi, -\dot{\phi}), \tag{34}$$

rendering it sufficient to consider only half of the parameter space with $\dot{\phi}_B > 0$. Here, ϕ_B can assume any value in the range $|\phi_B| \leq \phi^I_{\rm max} = \sqrt{2\rho^I_c}/m$, where $\phi^I_{\rm max}$ is determined by $V(\phi^I_{\rm max}) = \rho^I_c$ [46].

For any chosen initial condition ϕ_B with $\dot{\phi}_B > 0$, which yields approximately 60 e-folds [cf. Figure 3], we numerically solve the dynamical Equations (7)–(10), and find that the evolution of the universe in the post-bounce regime ($t \geq 0$) can always be divided

into three different phases, *bouncing, transition, and inflation*, as shown in Figure 1. In Figure 2, three numerical solutions are shown together with the analytical solution given by Equation (26) during the bouncing phase, $t \in (0, 10^4)\ t_{\rm pl}$. Note that the universal behavior of the evolution of the universe during the bouncing phase does not depend on the specific choice of ϕ_B, as long as the kinetic-energy-dominated condition (1) is satisfied at the bounce [46].

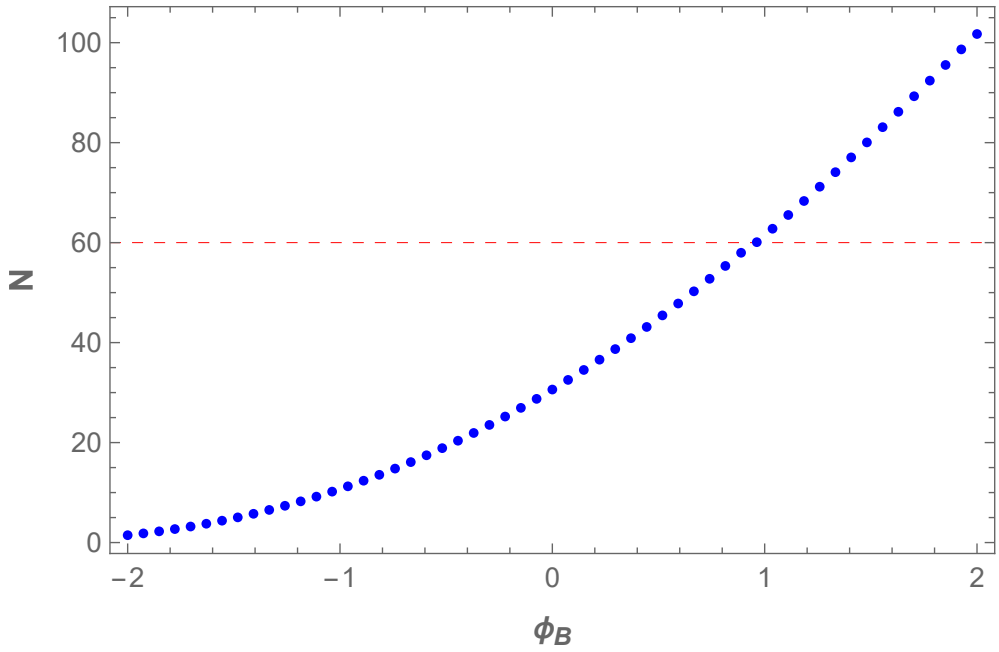

Figure 3. The e-folds N during the inflationary period for the chaotic potential (33) with $m = 1.26 \times 10^{-6}\ m_{pl}$ for $\dot{\phi}_B > 0$. The case $\dot{\phi}_B < 0$ can be obtained by the symmetry $(\phi, \dot{\phi}) \to (-\phi, -\dot{\phi})$, a particular property owned by this model.

With the same initial conditions imposed at the bounce, we numerically solve the dynamic Equations (7)–(10) for $t \leq 0$ and obtain the solutions in the pre-bounce regime. In Figure 4a, the corresponding equation of state $w(t)$ defined by Equation (25) is plotted. From this figure, we can see that the evolution of the universe in the pre-bounce phase can also be *universally* divided into three different phases:

$$\begin{aligned} &(i)\ pre-bouncing\ (w(t) \simeq 1), \\ &(ii)\ pre-transition\ (-1 < w(t) < 1), \\ &(iii)\ pre-de\ Sitter\ (w(t) \simeq -1). \end{aligned} \tag{35}$$

The transition occurs at $t \simeq -10 t_{\rm pl}$ and is very rapid. From Figure 4b, we can see that this is because the kinetic energy of the scalar field decreases dramatically as time becomes increasingly negative and is soon dominated by its potential energy. In addition, the effective cosmological constant quickly dominates the evolution of the universe $\rho(t)/\rho_\Lambda \ll 1$, as shown in Figure 4c, whereby the Hubble parameter becomes a (negative) constant, and spacetime quickly approaches de Sitter. As a result, the pre-bouncing phase is also very short compared to the pre-de Sitter phase.

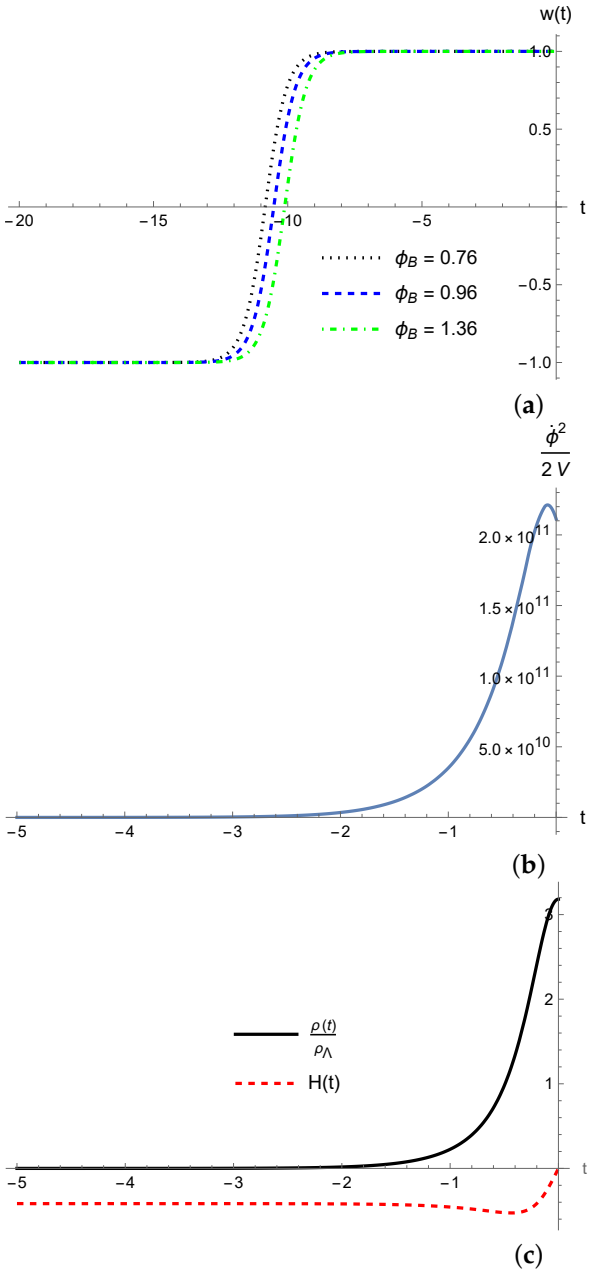

Figure 4. (**a**) The evolution of the equation of state in the pre-bounce phase for the chaotic potential with various choices of ϕ_B for $\dot{\phi}_B > 0$. (**b**) Ratio between the kinetic energy and potential of the scalar field. (**c**) The ratio $\rho(t)/\rho_\Lambda$ between the energy density of the scalar field and the effective cosmological constant, together with the Hubble parameter $H(t)$.

In Figure 5, the numerical solutions of $a(t)$ and $\phi(t)$ are plotted for three different initial conditions, which all satisfy (1). Form this figure, it can be seen that the numerical solutions are indistinguishable. In fact, they remain indistinguishable not only across different initial conditions but also across various inflationary potentials, provided that the condition (1) holds at the bounce. This universality will be further demonstrated in the subsequent sections.

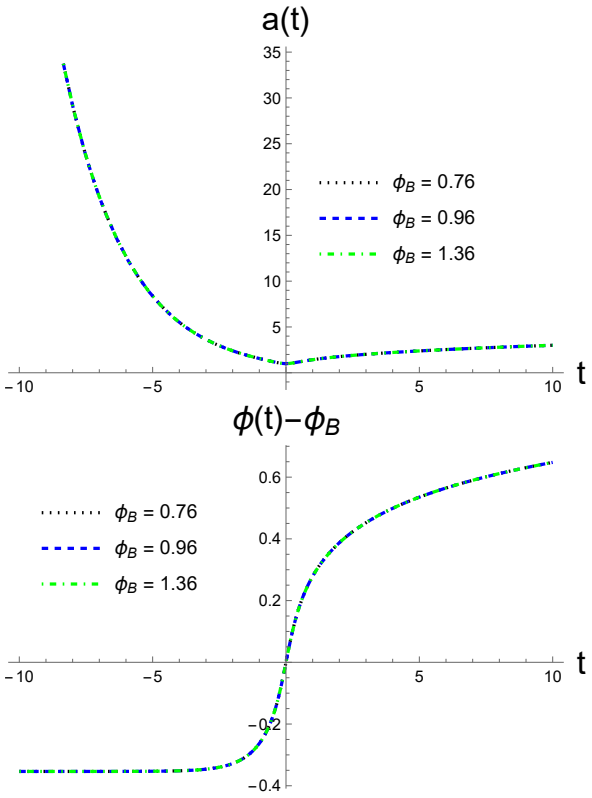

Figure 5. The numerical solutions of $a(t)$ and $\phi(t)$ for the chaotic potential with $\dot{\phi}_B > 0$. In the figures, the numerical curves with different initial conditions are indistinguishable.

3.2. Starobinsky Potential

The Starobinsky potential results from adding an R^2 term to the Einstein–Hilbert action [77]. After a conformal transformation, in the Einstein frame, the theory is equivalent to a scalar field with the potential [78]

$$V(\phi) = \frac{3m^2}{32\pi G}\left(1 - \exp\left(-\sqrt{\frac{16\pi G}{3}}\phi\right)\right)^2, \tag{36}$$

where the mass is set to $2.49 \times 10^6\ m_{\rm pl}$ [2]. Unlike the case with chaotic potential, now the slow-roll inflation can take place only when $\phi > \phi_{\rm end} \simeq 0.188\ m_{\rm pl}$ [46].

In addition, the Starobinsky potential does not share the symmetry of the chaotic one, given by Equation (34). Therefore, in the following, we consider both $\dot{\phi}_B > 0$ and $\dot{\phi}_B < 0$ separately. In particular, in Figure 6 we plot the e-fold N of inflation defined by Equation (32) vs. different initial conditions ϕ_B for $\dot{\phi}_B > 0$ and $\dot{\phi}_B < 0$, respectively.

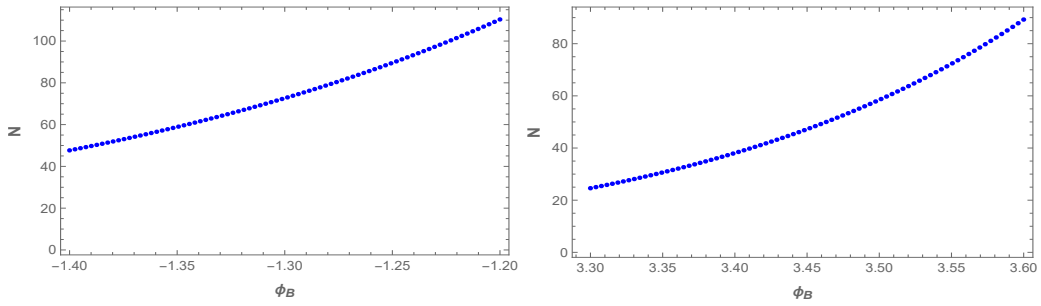

Figure 6. E-folds produced during slow inflation for different values of ϕ_B for the Starobinsky potential (36). **Left-panel**: $\dot{\phi}_B > 0$. **Right-panel**: $\dot{\phi}_B < 0$.

To confirm the universality of the evolution of the universe during the post-bounce regime ($t \geq 0$), in Figure 7 we plot out $a(t)$ and $\phi(t)$ with the initial conditions

$$\phi_B = \begin{cases} 1.38, \ -1.40, \ -1.45, & \dot{\phi}_B > 0, \\ 3.45, \quad 3.47, \quad 3.51, & \dot{\phi}_B < 0, \end{cases} \tag{37}$$

so that during slow-roll inflation, about 60 e-folds can be produced.

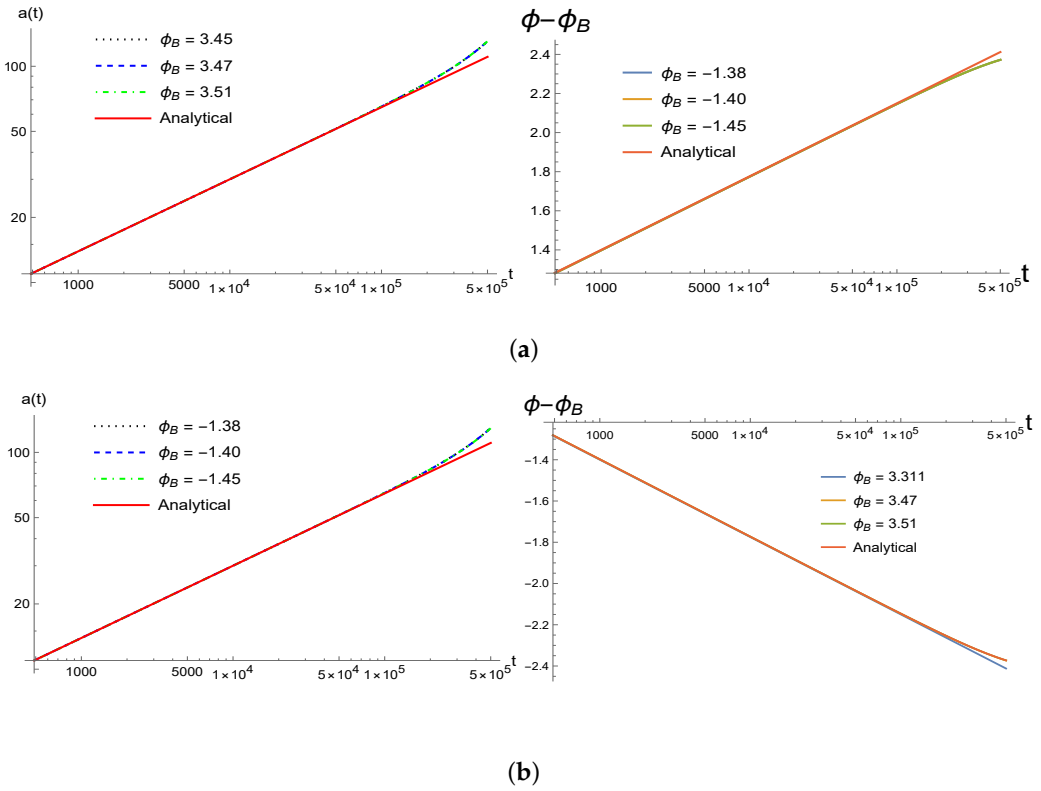

Figure 7. The numerical solutions $a(t)$ and $\phi(t)$ with indicated initial conditions for the Starobinsky potential (36) in the post-bounce regime ($t > 0$), where (**a**) For $\dot{\phi}_B > 0$, and (**b**) for $\dot{\phi}_B < 0$. To compare with the analytical solutions given by Equation (26), we also plot them out, denoted by the red solid lines.

On the other hand, with the same initial conditions as those chosen in Figure 7, we plot the equation of state $w(t)$ in the post-bounce ($t \geq 0$) and the pre-bounce ($t \leq 0$) regimes in Figure 8. From these figures, it can be clearly seen that in the post-bounce regime, three different phases defined by Equation (24) exist. The only difference from the chaotic potential case is that the transition phase now occurs at approximately $t \simeq 10^5 \ t_{\rm pl}$, instead of $t \simeq 10^4 \ t_{\rm pl}$ as shown in Figure 1.

Equally remarkable, the evolution of the universe in the pre-bounce regime ($t \leq 0$) is also universally divided into three phases defined by Equation (35). However, the time t_m defined by $\dot{H}(t_m) \simeq 0$ in the pre-transition phase weakly depends on the initial values of ϕ_B but can be significantly different with different signs of $\dot{\phi}_B$, as shown in Figure 8, where $t_m \simeq -5t_{\rm pl}$ for $\dot{\phi}_B > 0$, and $t_m \simeq -10.5t_{\rm pl}$ for $\dot{\phi}_B < 0$.

In Figure 9, the numerical solutions of $a(t)$, $\phi(t)$ for several different choices of initial conditions ϕ_B with $\dot{\phi}_B > 0$ and $\dot{\phi}_B < 0$ are plotted out, respectively. From the figures we can see that the scalar field $\phi(t)$ quickly approaches a constant, which is negative for $\dot{\phi}_B > 0$ and positive for $\dot{\phi}_B < 0$.

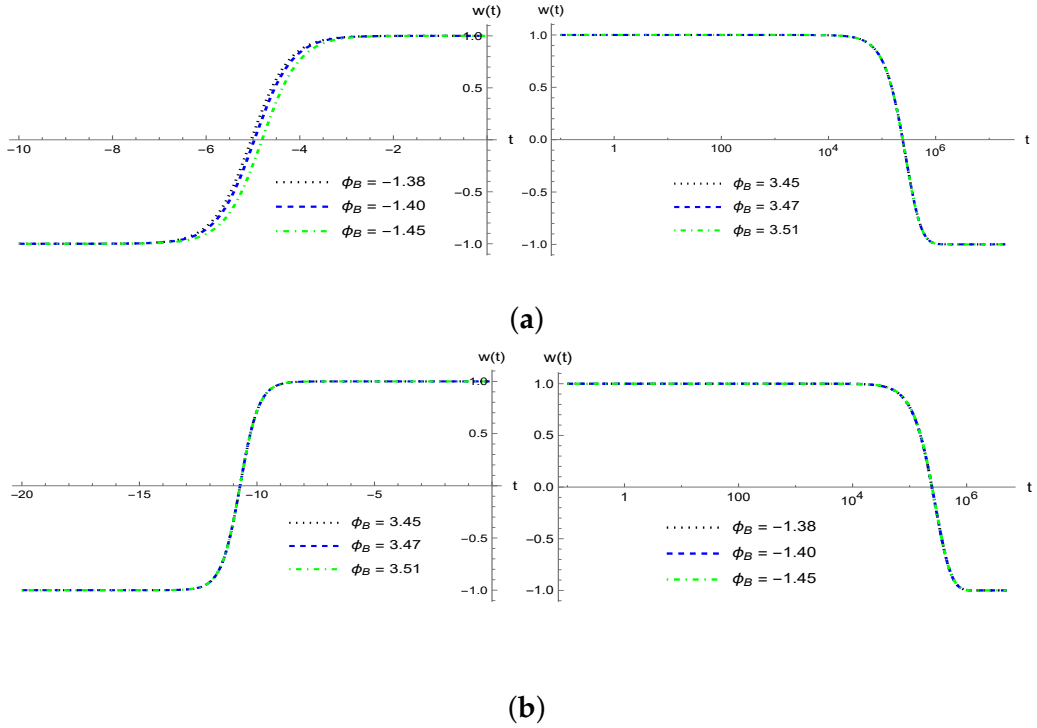

Figure 8. The equation of state for the Starobinsky potential (36) for different values of ϕ_B that result in greater than 50 e-Folds for (**a**) $\dot{\phi}_B > 0$ and (**b**) $\dot{\phi}_B < 0$.

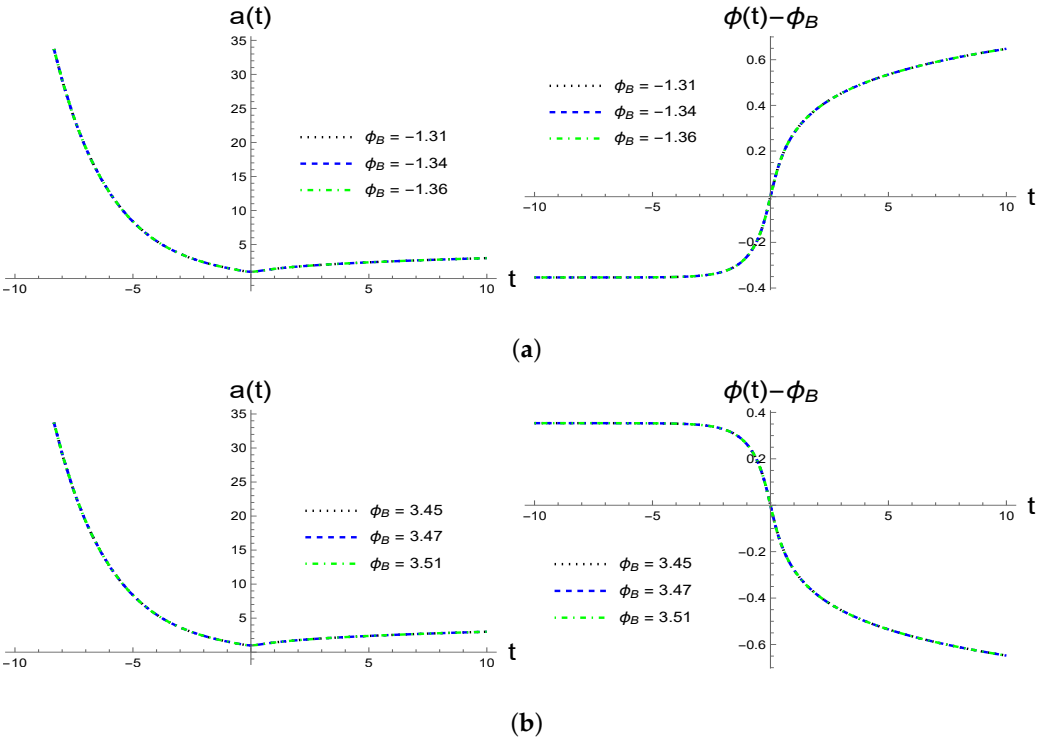

Figure 9. The numerical solutions of $a(t)$ and $\phi(t)$ with various initial values of ϕ_B for the Starobinsky potential (36), where (**a**) for $\dot{\phi}_B > 0$ and (**b**) For $\dot{\phi}_B < 0$.

3.3. α-Attractor Potentials

The α-attractor potentials usually take several different forms [2]. In this subsection, we consider several representative cases.

3.3.1. Generalized Starobinsky Potentials

One type of α-attractor potential derived from supergravity takes the form [79]

$$V(\phi) = V_0\left(1 - e^{-\frac{\phi}{\sqrt{6\alpha}}}\right)^2, \tag{38}$$

which is often referred to as the generalized Starobinsky potentials or E-models [73]. For $\alpha = \sqrt{9/(8\pi G)}$, the above potentials are precisely reduced to the Starobinsky potential given by Equation (36).

In the following, we consider the case $\alpha = 0.0962$ with $V_0 = 10^{-12}$ GeV. We then find that the initial values of ϕ_B for both $\dot{\phi}_B > 0$ and $\dot{\phi}_B < 0$, with which the e-fold N is always no less than 45, as shown in Figure 10. Using several such values of ϕ_B, the corresponding equation of state $w(t)$ for both $\dot{\phi}_B > 0$ and $\dot{\phi}_B < 0$ is plotted out in Figure 11. From these figures, we can see that each of the post-bounce and pre-bounce regimes can be universally divided into three phases, as given in Equations (24) and (35).

In Figure 12, we plot the numerical solutions of $a(t)$ and $\phi(t)$ for several initial values of ϕ_B for $\dot{\phi}_B > 0$ and $\dot{\phi}_B < 0$, respectively. From these figures, it can be seen that, similar to the previous cases, the numerical solutions are almost indistinguishable from each other.

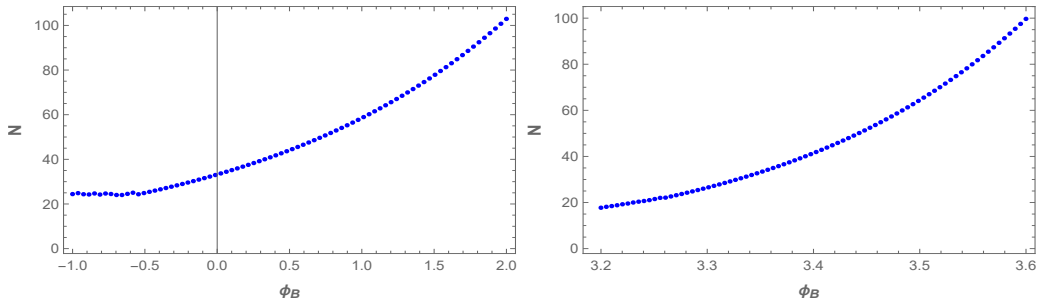

Figure 10. E-folds for different values of ϕ_B for the generalized Starobinsky potentials (38) with $\alpha = 0.0962$ and $V_0 = 10^{-12}$ GeV.

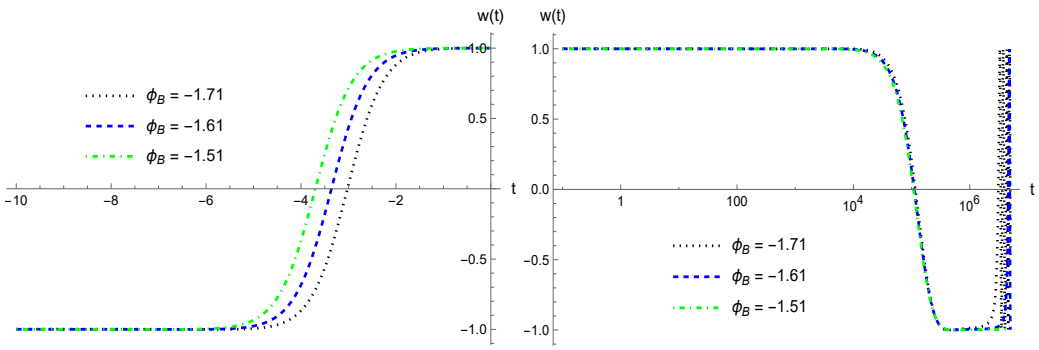

(a)

Figure 11. *Cont.*

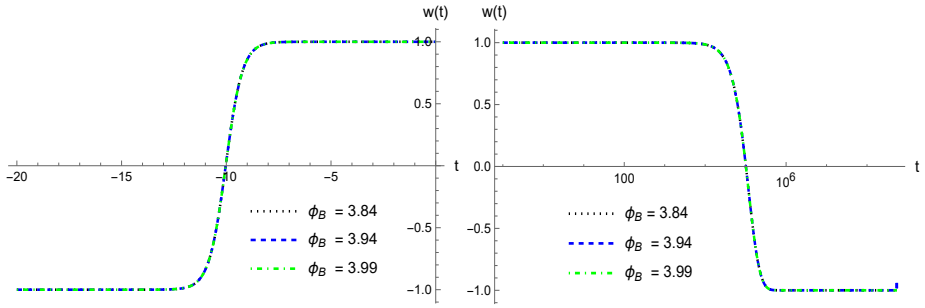

(**b**)

Figure 11. The equation of state for the generalized Starobinsky potentials (38) for different values of ϕ_B that result in at least 50 e-Folds with $\alpha = 0.0962$ and $V_0 = 10^{-12}$ GeV, where (**a**) for $\dot{\phi}_B > 0$ and (**b**) for $\dot{\phi}_B < 0$.

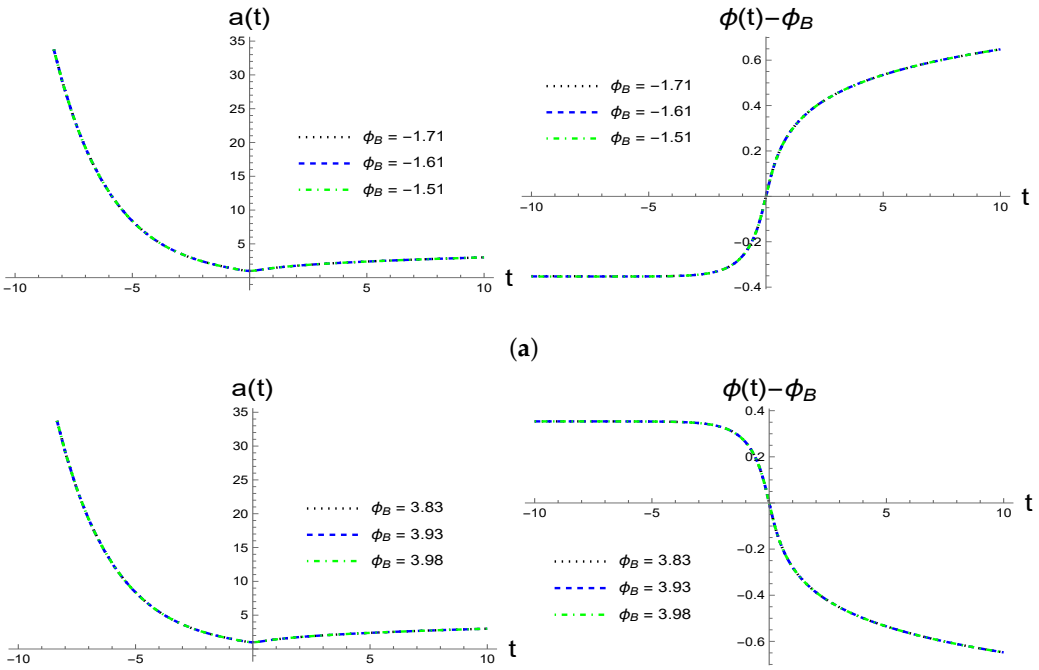

(**a**)

(**b**)

Figure 12. The numerical solutions of $a(t)$ and $\phi(t)$ for the generalized Starobinsky potentials (38) with $\alpha = 0.0962$ and $V_0 = 10^{-12}$ GeV. (**a**) For $\dot{\phi}_B > 0$, and (**b**) for $\dot{\phi}_B < 0$.

3.3.2. Polynomial of the First Kind

The polynomial potential of the first kind takes the form [73]

$$V(\phi) = V_0 \frac{\phi^4}{\phi^4 + \mu^4}, \tag{39}$$

where V_0 and μ are two constants. In this paper, we take the values of V_0 and μ as $V_0 = 3.3787 \times 10^{-15}$ GeV and $\mu = 0.31075$ [80].

Note that, similar to the chaotic potential, now the polynomial potential of the first kind has the symmetry

$$V(\phi) = V(-\phi). \tag{40}$$

As a result, the case with $\dot{\phi}_B < 0$ can be obtained from the case with $\dot{\phi}_B > 0$ via the symmetry (34). This is clearly true for all the cases with the above symmetry, including the polynomial potential of the second kind and the generalized T-models to be considered below. Therefore, in all these cases, we shall consider only the cases with $\dot{\phi}_B > 0$.

In Figures 13 and 14, we then plot the e-fold N and the equation of state $w(t)$ for $\dot{\phi}_B > 0$. Similar to the previous cases, the evolution of the universe in each of the pre- and post-bounce regimes can be universally divided into three epochs, described by Equations (24) and (35), respectively. In Figure 15, we plot the functions $a(t)$ and $\phi(t)$ with various initial values of ϕ_B for $\dot{\phi}_B > 0$.

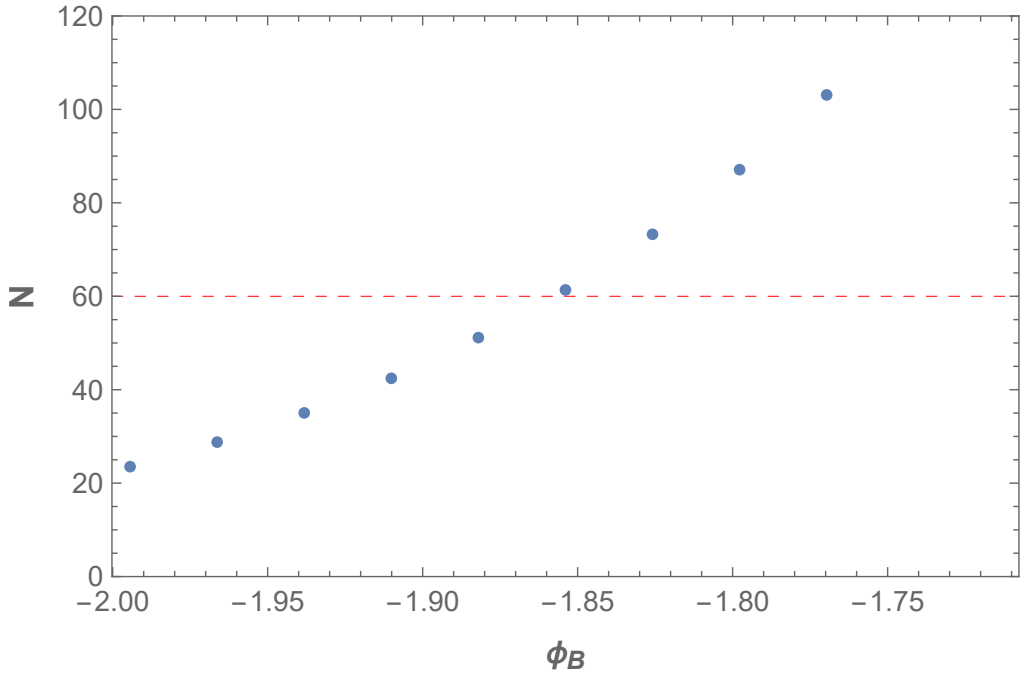

Figure 13. E-fold N for $\dot{\phi}_B > 0$ with different values of ϕ_B for the polynomial potential of the first kind given by Equation (39) where $V_0 = 3.3787 \times 10^{-15}$ GeV and $\mu = 0.31075$. The case with $\dot{\phi}_B < 0$ can be obtained by the symmetry (34).

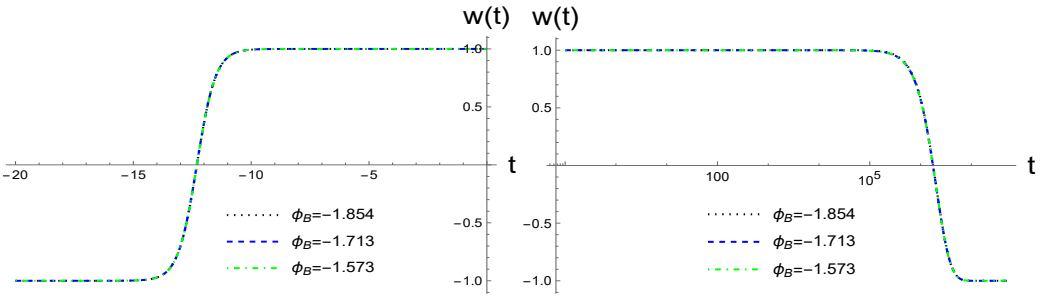

Figure 14. The equation of state $w(t)$ for the polynomial potential of the first kind given by Equation (39) with $\dot{\phi}_B > 0$ and different values of ϕ_B, where $V_0 = 3.3787 \times 10^{-15}$ GeV and $\mu = 0.31075$.

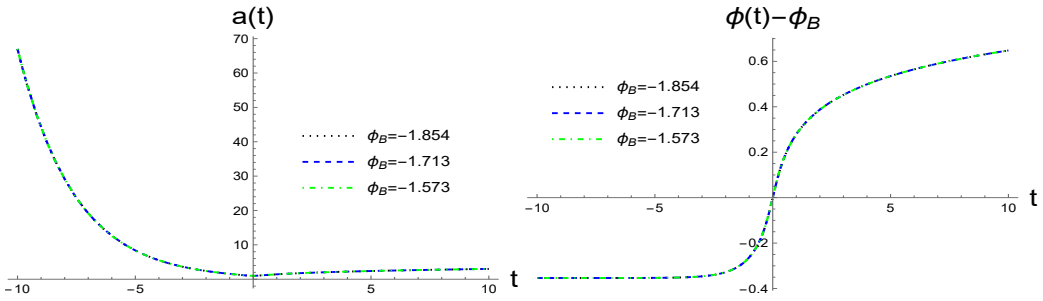

Figure 15. The numerical solutions of $a(t)$ and $\phi(t)$ with different initial values of ϕ_B for the polynomial potential of the first kind given by Equation (39) with $\dot{\phi}_B > 0$, where $V_0 = 3.3787 \times 10^{-15}$ GeV and $\mu = 0.31075$.

3.3.3. Polynomial of the Second Kind

The polynomial potential of the second kind is given by [73]

$$V(\phi) = V_0 \frac{\sqrt{\phi^2 + \mu^2} - \mu}{\sqrt{\phi^2 + \mu^2} + \mu}. \tag{41}$$

In this paper, we adopt the best fitting values of V_0 and μ with current observations given by $V_0 = 3.2599 \times 10^{-15}$ and $\mu = 0.01043$ [80].

In Figures 16 and 17, we plot $N(\phi_B)$ and the corresponding equation of state $w(t)$ for several initial conditions ϕ_B for $\dot{\phi}_B > 0$. These values of ϕ_B guarantee that the e-folds during inflation will be about 60, as shown in Figure 16. On the other hand, Figure 17 shows again that the evolution of the universe in each of the pre- and post-bounce regimes can be universally divided into three different epochs.

In Figure 18, we plot numerical solutions of $a(t)$ and $\phi(t)$. Again, these numerical solutions are almost indistinguishable with different initial conditions as specified in the figures, which show again the universality of the evolution of the Universe.

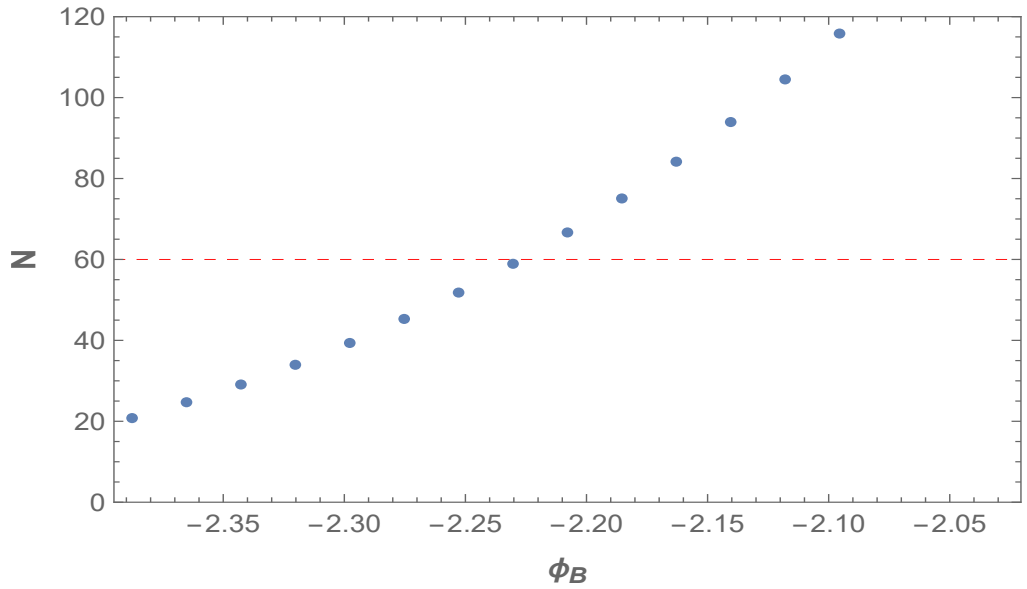

Figure 16. E-fold N for different values of ϕ_B for the polynomial potential of the second kind given by Equation (41) with $\dot{\phi}_B > 0$, $V_0 = 3.2599 \times 10^{-15}$ GeV and $\mu = 0.01043$.

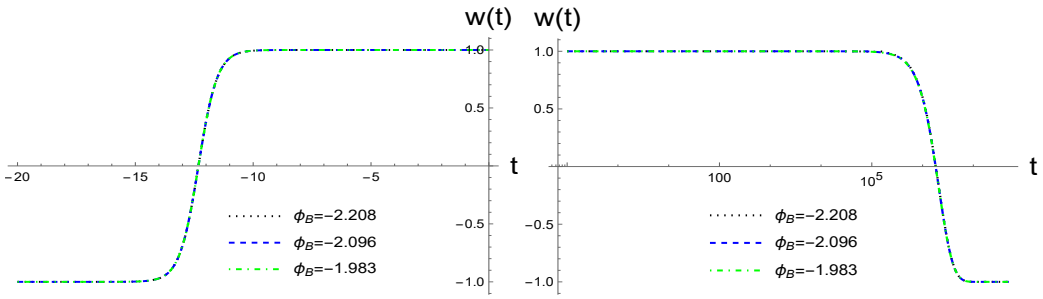

Figure 17. The equation of state $w(t)$ with different values of ϕ_B for the polynomial potential of the second kind given by Equation (41) with $\dot{\phi}_B > 0$, $V_0 = 3.2599 \times 10^{-15}$ GeV and $\mu = 0.01043$.

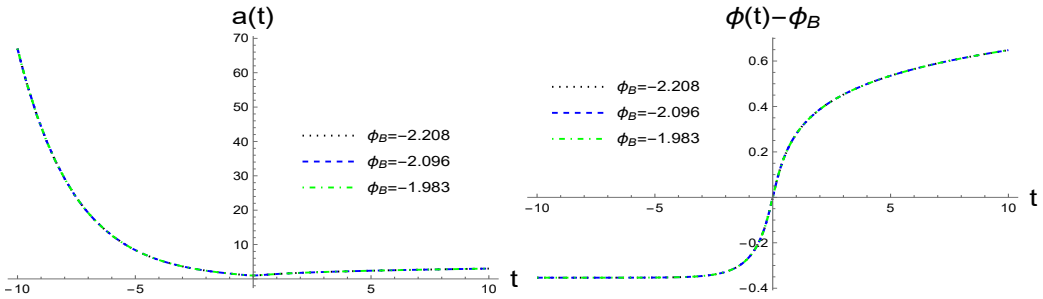

Figure 18. The numerical and analytical solutions of $a(t)$ and $\phi(t)$ with different initial values of ϕ_B for $\dot{\phi}_B > 0$ and the polynomial potential of the second kind given by Equation (41), where $V_0 = 3.2599 \times 10^{-15}$ GeV and $\mu = 0.01043$.

3.3.4. Generalized T-Models

The generalized T-model potentials of the superconformal inflationary models are given by [81]

$$V(\phi) = V_0 \tanh^2\left(\frac{\phi}{\sqrt{6\alpha}}\right), \tag{42}$$

where the best fitting values of V_0 and α with current cosmological observations are given by $V_0 = 1.96 \times 10^{-15}$ and $\alpha = 0.0962$ [80].

In Figures 19 and 20, we plot $N(\phi_B)$ and the corresponding equation of state $w(t)$ for several initial conditions ϕ_B with $\dot{\phi}_B > 0$. These values of ϕ_B also guarantee that the e-folds of the expansions of the universe during the inflationary period will be about 60, as shown in Figure 20. On the other hand, Figure 20 shows again that the evolution of the universe in each of the pre- and post-bounce regimes can be universally divided into three different epochs, as described by Equation (24) in the post-bounce regime and by Equation (35) in the pre-bounce regime.

In Figure 21, we plot the numerical solutions of $a(t)$ and $\phi(t)$ with several initial conditions for $\dot{\phi}_B > 0$, which all satisfy the condition (1) at the bounce. Again, they show the universality of the solutions.

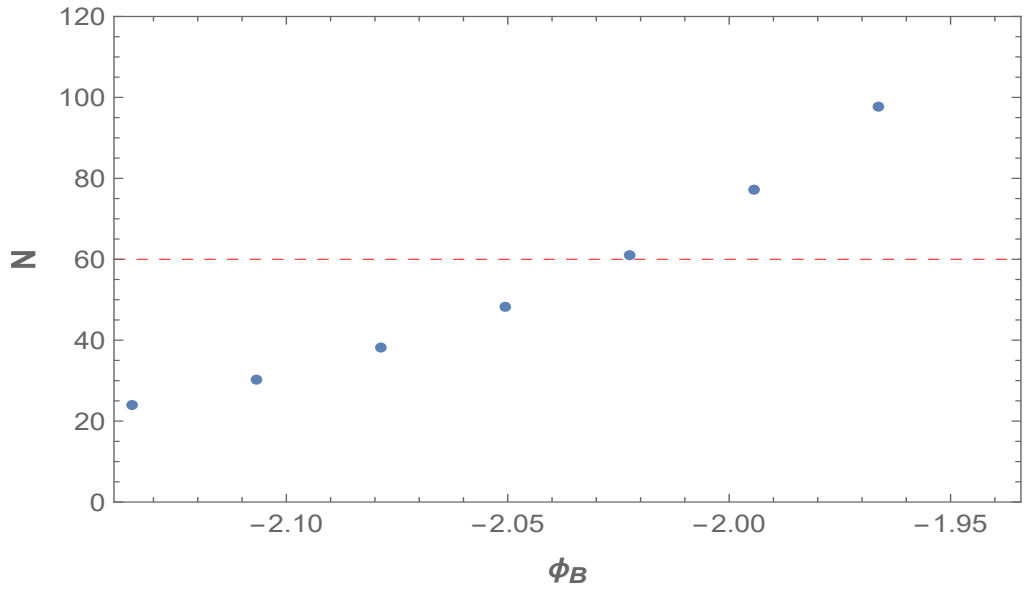

Figure 19. E-folds N for the generalized T-Models given by (42) with $\dot{\phi}_B > 0$, $V_0 = 1.96 \times 10^{-15}$ and $\alpha = 0.0962$.

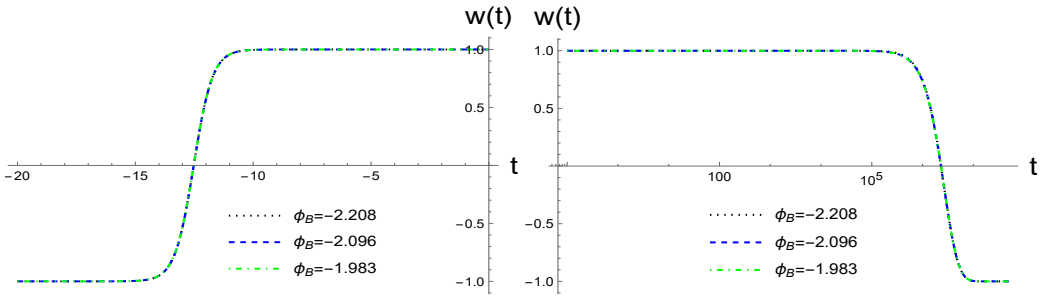

Figure 20. The equation of state $w(t)$ with different values of ϕ_B for the the generalized T-Models given by (42) with $\dot{\phi}_B > 0$, $V_0 = 1.96 \times 10^{-15}$ and $\alpha = 0.0962$.

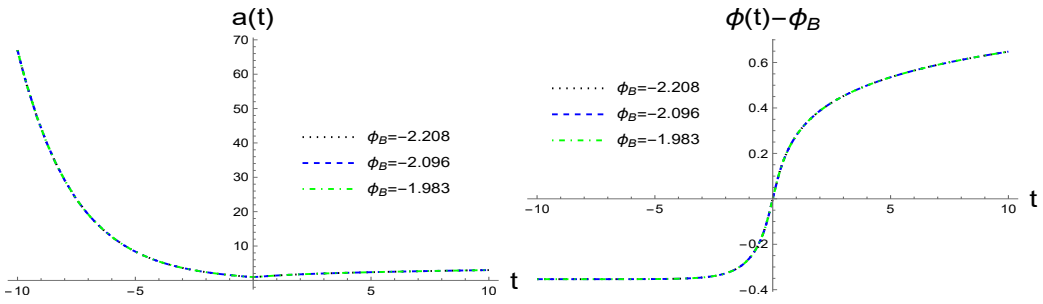

Figure 21. The numerical solutions of $a(t)$ and $\phi(t)$ for various initial conditions of ϕ_B for the generalized T-Models given by (42) with $\dot{\phi}_B > 0$, $V_0 = 1.96 * 10^{-15}$ and $\alpha = 0.0962$.

3.4. Natural Inflation

The natural inflationary potential, motivated by the concept of a pseudo-Nambu–Goldstone boson, takes the form [82],

$$V(\phi) = \Lambda^4 \left[1 + \cos\left(\frac{\phi}{\mu}\right)\right], \tag{43}$$

where $\mu \equiv f/\mathcal{N}$, $\Lambda \simeq m_{\rm GUT} \simeq 10^{16}$ GeV, $f \simeq m_{\rm pl}$, and $\mathcal{N}$ is a dimensionless constant. Because of the periodic property of the potential, without loss of generality, we can restrict ourselves only to the region

$$-\pi \leq \frac{\phi}{\mu} \leq \pi. \tag{44}$$

In addition, the potential is also symmetric under the replacement $\phi \to -\phi$. So, in this case it is also sufficient to consider only the case $\dot{\phi}_B > 0$. In the following, we consider only two representative cases, $\mu/\ m_{\rm pl} = (1,\ 5)$.

3.4.1. $\mu = m_{\rm pl}$

In this subsection, we first identify the initial conditions ϕ_B for both $\dot{\phi}_B > 0$ and $\dot{\phi}_B < 0$, with which the e-folds of inflation are approximately 60. In Figure 22, we show two sets of such data. Note that the number of such sets is infinitely large because the potential is now a periodic function of ϕ. With some of the initial conditions presented in Figure 22, we plot the corresponding equation of state $w(t)$ in Figure 23, which again shows the universal properties described by Equations (24) and (35). The corresponding numerical solutions of $a(t)$ and $\phi(t)$ are given in Figure 24 for $\dot{\phi}_B > 0$ and $\dot{\phi}_B < 0$, respectively.

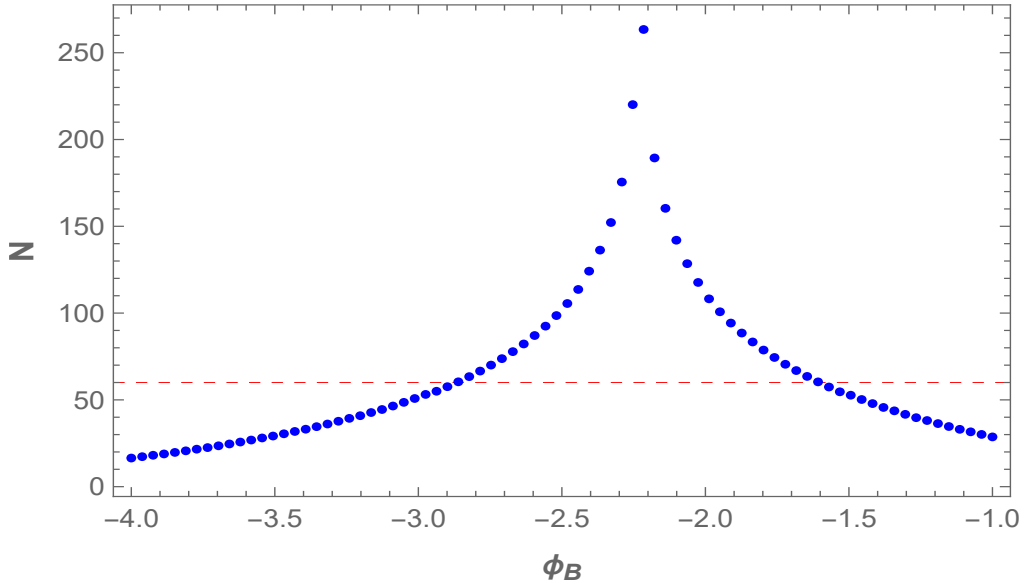

Figure 22. E-folds of natural inflation with the potential given by Equation (43), $\dot{\phi}_B > 0$, $\Lambda = 10^{16}$ GeV, and $\mu = m_{\rm pl}$ for different values of the initial conditions ϕ_B.

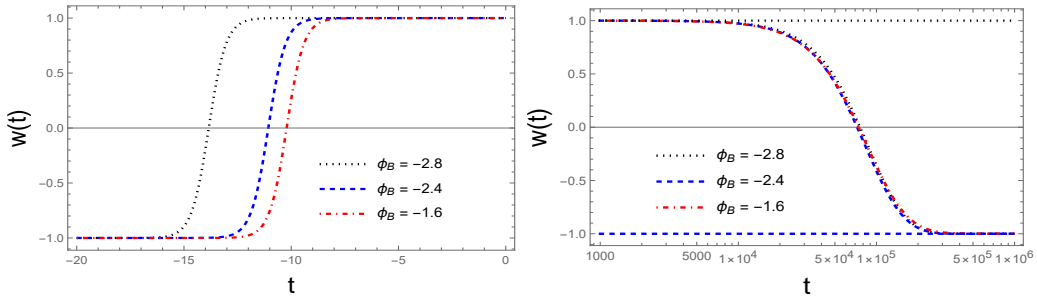

Figure 23. The equation of state $w(t)$ with different values of ϕ_B for the natural inflation with the potential given by Equation (43), $\dot{\phi}_B > 0$, $\Lambda = 10^{16}$ GeV and $\mu = 1\ m_{\rm pl}$.

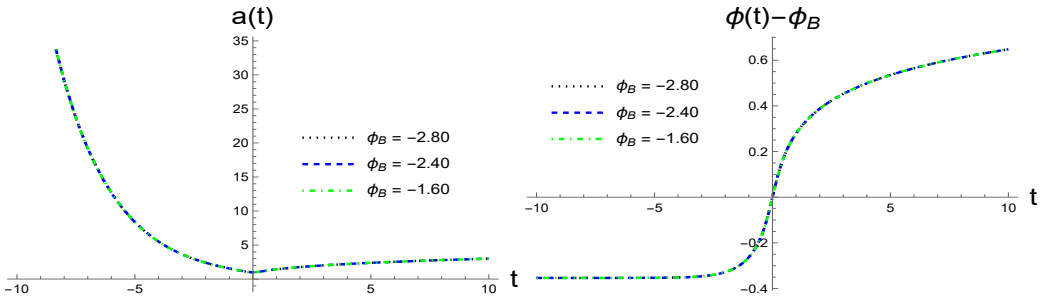

Figure 24. The numerical solutions of $a(t)$ and $\phi(t)$ for various initial conditions of ϕ_B for the natural inflation with the potential given by Equation (43), $\dot{\phi}_B > 0$, $\Lambda = 10^{16}$ GeV and $\mu = 1\ m_{\rm pl}$.

3.4.2. $\mu = 5\ m_{\rm pl}$

In this case, in Figure 25 we plot the e-folds of the natural inflation for both $\dot{\phi}_B > 0$ and $\dot{\phi}_B < 0$, whereby we can read off the initial conditions of ϕ_B for which the inflation will last about 60 e-folds. Then, with several choices of such initial values of ϕ_B presented in Figure 25, the equation of state $w(t)$ is plotted in Figure 26. Again, we can clearly identify the three distinguishable epochs in each of the pre- and post-bounce regimes. The corresponding numerical solutions of $a(t)$ and $\phi(t)$ are plotted in Figure 27 for both $\dot{\phi}_B > 0$ and $\dot{\phi}_B < 0$.

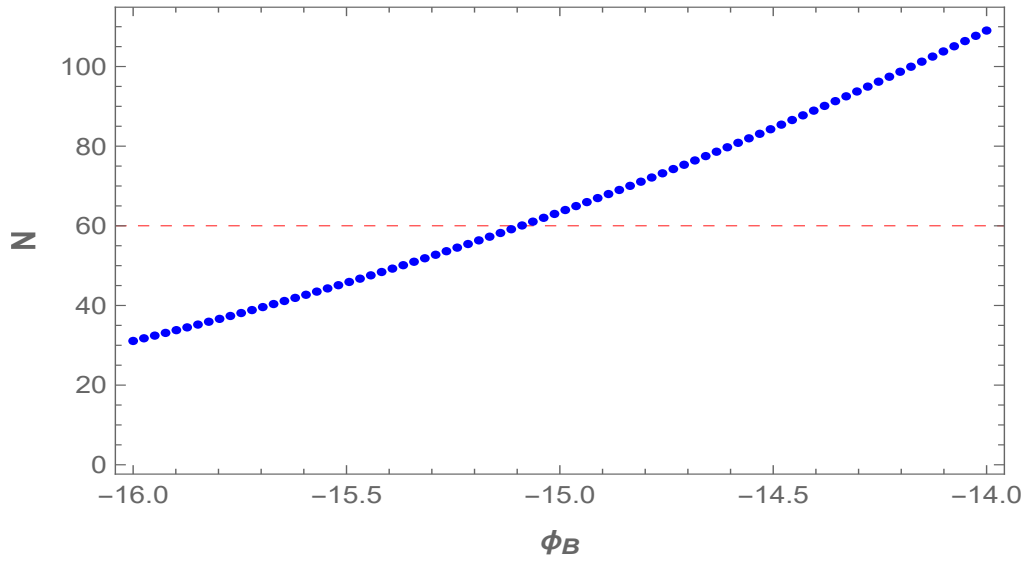

Figure 25. E-folds of natural inflation with the potential given by Equation (43), $\dot{\phi}_B > 0$, $\Lambda = 10^{16}$ GeV and $\mu = 5\ m_{\rm pl}$ for different values of the initial conditions ϕ_B.

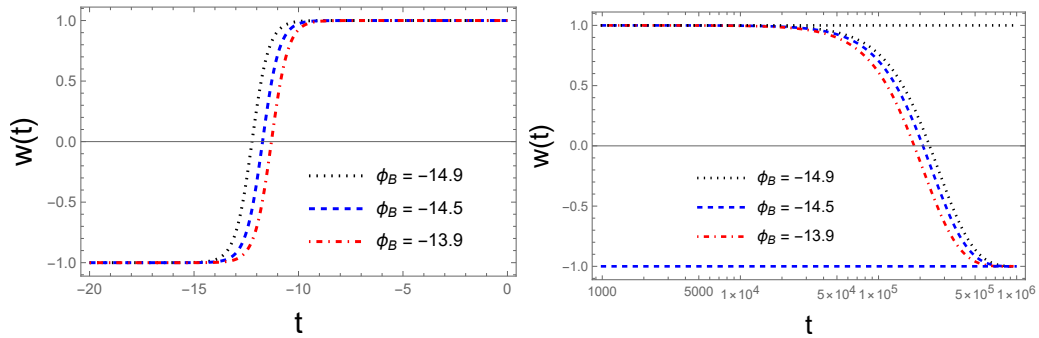

Figure 26. The equation of state $w(t)$ with different values of ϕ_B for the natural inflation with the potential given by Equation (43), $\dot{\phi}_B > 0$, $\Lambda = 10^{16}$ GeV and $\mu = 5\ m_{\rm pl}$.

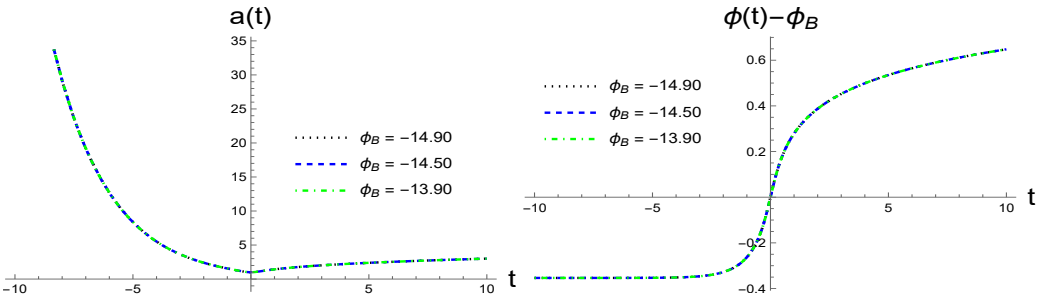

Figure 27. The numerical solutions of $a(t)$ and $\phi(t)$ for various initial conditions of ϕ_B with $\dot{\phi}_B > 0$ for natural inflation with the potential given by Equation (43), $\dot{\phi}_B > 0$, $\Lambda = 10^{16}$ GeV and $\mu = 5\, m_{\rm pl}$.

4. Analytical Solutions for the Evolution of the Universe

As shown previously [46], the evolution of the Universe in the post-bounce regime ($t \geq t_B$) is universal, and can be divided into three different epochs, as defined in Equation (24). In addition, during the bouncing phase, the solutions of $a(t)$ and $\phi(t)$ are given by the analytical solutions of Equation (26) [see Figure 2].

In this section, we aim to show that this is also the case in the pre-bounce regime ($t \leq t_B$). To demonstrate this, let us first plot the numerical solutions of $a(t)$ and $\phi(t)$ together for all the cases considered in the last section. Since for each potential the numerical solutions are indistinguishable for different initial values of ϕ_B, we plot only one solution for each model. In addition, to highlight any potential differences between the models, we group them into two categories: one comprising chaotic, Starobinsky, and natural inflationary potentials, and the other containing the first- and second-kind polynomials and the generalized T-models. Despite this grouping, the solutions are indistinguishable across all models, as illustrated in Figure 28, where the right-hand and left-hand panels correspond to the two groups, respectively. The numerical solutions of $a(t)$ are independent of the signs of $\dot{\phi}_B$ and are given by Figure 28a, while The numerical solutions of $\phi(t)$ depend on the signs of $\dot{\phi}_B$ and are given, respectively, by Figure 28b,c. From Figure 28a, we can see that the Universe soon enters the pre-de Sitter phase, and $a(t)$ increases exponentially $a(t) \propto e^{-H_\Lambda t}$ as t becomes increasingly negative, where $H_\Lambda \equiv \sqrt{8\pi\alpha G\rho_\Lambda/3}$ [cf. Equation (21)]. In contrast, the evolution of the scalar field indeed depends on the signs of $\dot{\phi}_B$, as in the post-bounce regime, as can be seen from Equation (26). In particular, it quickly approaches a negative constant for $\dot{\phi}_B > 0$ and a positive constant for $\dot{\phi}_B < 0$, as shown explicitly in Figure 28b,c.

To analytically model the expansion factor $a(t)$ in the pre-bounce regime, we find that it is convenient to assume that it takes the form

$$a(t) = \begin{cases} \left(1 + d_0\rho_c^I t^2\right)^{\frac{1}{6}} \sum_{n=2}^{4} d_n t^n, & t_m \leq t \leq t_B, \\ a(t_m)\exp\{-H_\Lambda(t - t_m)\}, & t \leq t_m, \end{cases} \tag{45}$$

where t_m is determined by $\dot{H}(t_m) \simeq 0$, and d_n $(n = 0, \ldots, 4)$ are fitting constants, which must satisfy the junction conditions at both the bounce ($t = 0$) and the turning point ($t = t_m$). In particular, we require that $a(t)$ *and its first derivative be contiguous across these two points*, where $a(t)$ is given by Equation (26) in the post-bounce regime ($t \geq 0$). As shown by Figure 28, the curve of $a(t)$ weakly depends on the initial values of ϕ_B and the inflationary potentials, so we can fit Equation (45) with any given inflationary potential and initial values of ϕ_B, as long as the condition (1) is satisfied. In particular, for the Starobinsky potential with $\dot{\phi}_B > 0$ we find

$$\begin{aligned} d_0 &\simeq 74.057, \quad d_2 \simeq 0.104, \\ d_3 &\simeq 0.001, \quad d_4 \simeq 0.002, \end{aligned} \tag{46}$$

for which the relative errors $\delta a(t)$ are less than 1% at any given moment $t \leq t_B$, as shown in Figure 29, where the relative errors are defined by

$$\delta A \equiv \left| \frac{A_n - A_a}{A_n} \right|, \tag{47}$$

where A_n and A_a denote the numerical and analytical values of A with $A = (a,\ \phi)$.

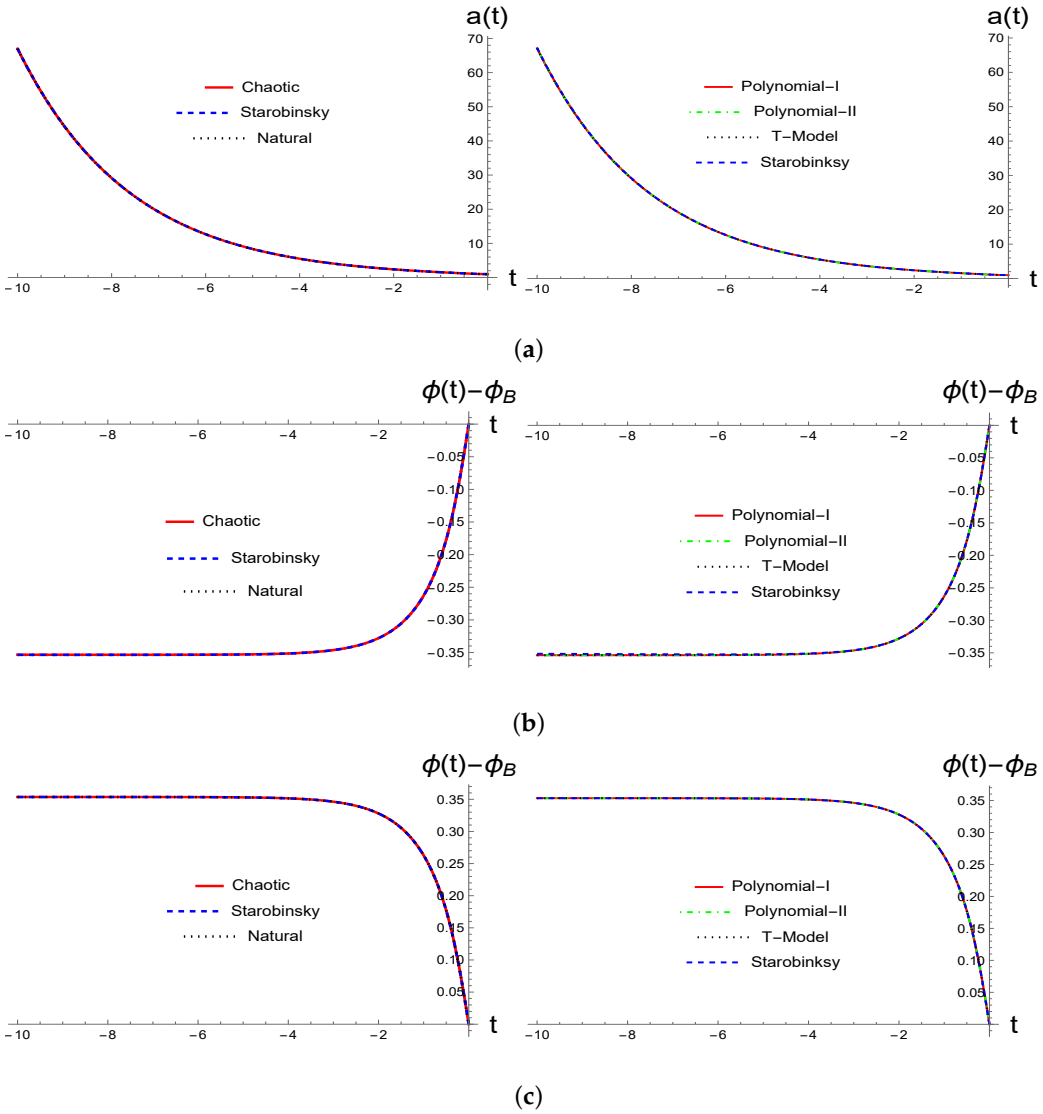

Figure 28. The numerical solutions of $a(t)$ and $\phi(t)$ for various potentials as specified in the figures. To see clearly the difference among the different models, we group the plot into two groups: **Left Panels**: Models with chaotic, Starobinsky, and natural inflationary potentials. **Right Panels**: Models with the polynomials of the first- and second kinds and the generalized T-models, although they are almost indistinguishable among all these models. (**a**) The evolution of the expansion factor $a(t)$ for both $\dot{\phi}_B > 0$ and $\dot{\phi}_B < 0$. (**b**) The evolution of the scalar field $\phi(t)$ for $\dot{\phi}_B > 0$. (**c**) The evolution of the scalar field $\phi(t)$ for $\dot{\phi}_B < 0$.

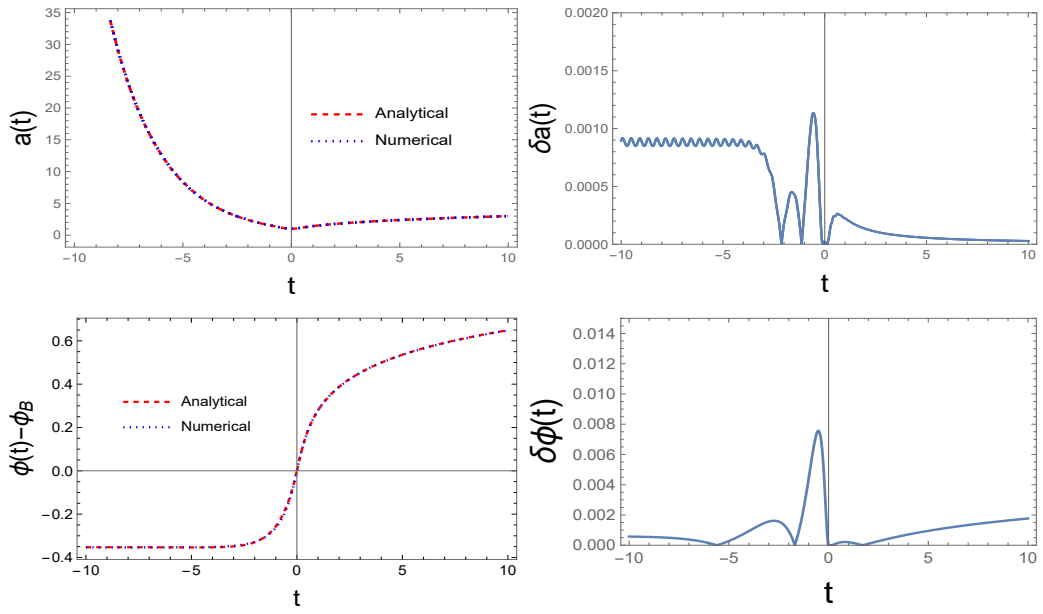

(**a**)

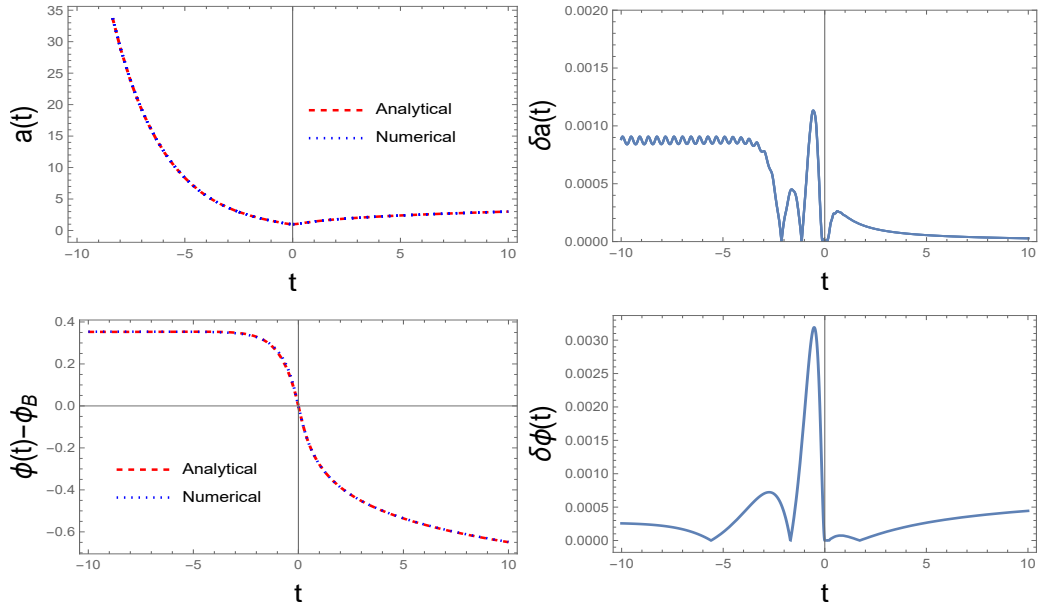

(**b**)

Figure 29. The numerical and analytical solutions of $a(t)$ and $\phi(t)$ with various initial values of ϕ_B for the Starobinsky potential (36), where (**a**) for $\dot{\phi}_B > 0$ and (**b**) For $\dot{\phi}_B < 0$. The analytical solutions are given by Equations (45)–(49).

In addition to model the scalar field $\phi(t)$, we find that in the whole pre-bounce regime ($t \leq t_B$), the scalar field can be cast in the form

$$\phi(t) - \phi_B = e_3 + \mathrm{sgn}(\dot{\phi}_B)(e_0 + e_2 t)e^{e_1 t}, \ (t \leq t_B), \tag{48}$$

where e_m $(m = 0, \ldots, 3)$ are the fitting constants. Again, we require that $\phi(t)$ *and its first derivative be continuous across the bounce*, where $\phi(t)$ is given by Equation (26) in the post-bounce regime ($t \geq t_B$). Then, fitting the above with the numerical data, we find that with the choices of fitting constants as

$$\begin{aligned} e_0 &\simeq 0.3526, \quad e_1 \simeq 0.9808, \\ e_2 &\simeq 0.0943, \quad e_3 \simeq -0.3526, \end{aligned} \tag{49}$$

for $\dot{\phi}_B > 0$, the relative errors $\delta\phi(t)$ are less than 1% at any given moment $t \leq t_B$, as shown in Figure 29. On the other hand, for $\dot{\phi}_B < 0$, the coefficients e_n are given by

$$\begin{aligned} e_0 &\simeq 0.3526, \quad e_1 \simeq 0.981, \\ e_2 &\simeq 0.094, \quad e_3 \simeq 0.3526. \end{aligned} \tag{50}$$

To understanding the above fitting results, let us first note that at the bounce $t = 0$ and at the remote contracting phase $t \to -\infty$, we have

$$\begin{aligned} 0 &= e_3 + \mathrm{sgn}(\dot{\phi}_B) e_0, \\ \phi_{-\infty} - \phi_B &= e_3, \end{aligned} \tag{51}$$

where $\phi_{-\infty} \equiv \phi(t = -\infty)$. On the other hand, from Figures 27 and 28, we also have $\phi_{-\infty} - \phi_B = -\mathrm{sgn}(\dot{\phi}_B)\mathcal{A}_0$, where $\mathcal{A}_0 \simeq 0.35326$. Thus, finally we have

$$e_0 = \mathcal{A}_0 \simeq 0.3526, \quad e_3 = -\mathrm{sgn}(\dot{\phi}_B)\mathcal{A}_0. \tag{52}$$

5. Conclusions and Remarks

In this paper, we systematically studied the evolution of the Universe before the quantum bounce ($t \leq t_B$) in one of the most promising modified theories of loop quantum cosmologies, namely mLQC-I [38]. This model can be derived from both bottom-up [39,42,43] and top-down [47–49] approaches, complementing recent studies focused on the post-bounce regime ($t \geq t_B$) [44–46], where t_B denotes the moment that the quantum bounce occurs, replacing the classical Big bang singularity. We specifically focused on the initial conditions where the kinetic energy of the inflationary field ϕ dominates the evolution of the Universe at the bounce $t = t_B$, as given by Equation (1). This set of initial conditions is important and leads generically to slow-roll inflation, as shown explicitly in [44–46]. Such considerations do not lose their generality, as slow-roll inflation is a generic feature in this model, as shown in [46].

With the above in mind, we examined several important inflationary potentials tested recently by the Planck 2018 data [2]. These include chaotic, Starobinsky, generalized Starobinsky, first- and second-order polynomials, generalized T-models, and natural inflation. Despite the fact that chaotic and natural inflationary models have some tensions with current observations [2], in this paper, we found that the evolution of the Universe weakly depends on the specific form of the potentials, as long as the initially kinetic-energy-dominated condition (1) holds at the quantum bounce.

In particular, we found that the evolution before the bounce can be universally divided into three different epochs: *the pre-bouncing, pre-transition, and pre-de Sitter epochs*, as defined in Equation (35). Although the exact moment of the transition point defined by $\dot{H}(t_m) = 0$ depends on the form of the inflationary potentials, the division of the above three different epochs is sharp and clear, as shown by the equation of state $w(\phi)$ in each of the cases considered in Section 3. In addition, the effective cosmological constant ρ_Λ defined in Equation (20) reaches Planck size and soon dominates the evolution of the Universe as one departs from the bounce to the deep contracting phase ($t \to -\infty$). Therefore, the pre-bouncing and pre-transition epochs are all very short compared to the pre-de Sitter epoch.

Moreover, the numerical solutions with the initial conditions that satisfy Equation (1) considered in all the models of this paper are universal, as shown explicitly by Figure 28, and can be approximated well by analytical solutions cast in the forms (45) for the expansion factor $a(t)$ and (48) for the inflation $\phi(t)$, where the constants d_n and e_n appearing in these expressions can be obtained by fitting the analytical solutions with the numerical ones. For the expansion factor $a(t)$, we have found that the fitting constants d_n are given by Equation (46)

for both $\dot{\phi}_B > 0$ and $\dot{\phi}_B < 0$. However, for the scalar field, the fitting constants e_n depend on the signs of $\dot{\phi}_B$, and are given, respectively, by Equations (49) and (50).

The above remarkable features are also shared in the evolution of the Universe in the post-bounce regime not only within the framework of mLQC-I [38,44–46] but also in the context of LQC [55–61]. We believe that this universal behavior of background evolution will significantly simplify future studies of cosmological perturbations in mLQC-I, as has already been demonstrated in LQC [56].

Author Contributions: Conceptualization, J.S., G.C. and A.W.; Methodology, R.P. and C.B. All authors have read and agreed to the published version of the manuscript.

Funding: A.W. is partially supported by the US NSF grant: PHY-2308845.

Data Availability Statement: No new data were created or analyzed in this study. Data sharing is not applicable to this article.

Acknowledgments: J.S. and C.B. are supported by the Baylor Physics graduate program, and R.P. (as a Baylor physics graduate student) and A.W. are partially supported by the US NSF grant: PHY-2308845.

Conflicts of Interest: The authors declare no conflict of interest.

Notes

1 The concept of a bouncing universe was inspired by string theory, first proposed in Ref. [20], and later studied intensively by various authors, see, for example Refs. [21–25] and references therein. Other bouncing models have been also studied extensively [26–31]. In this paper, we focus specifically on the quantum bounce from LQG, driven purely by quantum geometric effects.

2 It should be noted that such universal properties in the pre-bounce regime may not be shared by the standard LQC [54–61], as in LQC such an effective Planck-size cosmological constant is absent in the pre-bounce regime [12,16,18,19].

3 More precisely, it is symmetric for kinetic energy-dominated initial conditions $\dot{\phi}_B^2 \gg 2V(\phi_B)$ [12,38].

4 It is found that numerically it is more convenient to solve the dynamical Equations (7)–(10) than the ones of Equations (11), (12), (18) and (19), although they should give the same results. However, in the latter, the integration needs to be carried out in the pre- and post-bounce separately, and then connect them smoothly across the bounce.

References

1. Guth, A.H. Inflationary universe: A possible solution to the horizon and flatness problems. *Phys. Rev.* **1981**, *23*, 347–356. [CrossRef]
2. Akrami, Y.; Arroja, F.; Ashdown, M.; Aumont, J.; Baccigalupi, C.; Ballardini, M.; Banday, A.J.; Barreiro, R.B.; Bartolo, N.; Basak, S.; et al. Planck 2018 results. X. Constraints on inflation. *Astron. Astrophys.* **2020**, *641*, A10. [CrossRef]
3. Borde, A.; Guth, A.H.; Vilenkin, A. Inflationary space-times are incompletein past directions. *Phys. Rev. Lett.* **2003**, *90*, 151301. [CrossRef] [PubMed]
4. Green, M.B.; Schwarz, J.H.; Witten, E. *Superstring Theory: 25th Anniversary Edition*; Cambridge Monographs on Mathematical Physics; Cambridge University Press: Cambridge, UK, 2012.
5. Becker, K.; Becker, M.; Schwarz, J.H. *String Theory and M-Theory: A Modern Introduction*; Cambridge University Press: Cambridge, UK, 2006. [CrossRef]
6. Ashtekar, A.; Lewandowski, J. Background independent quantum gravity: A Status report. *Class. Quant. Grav.* **2004**, *21*, R53. [CrossRef]
7. Thiemann, T. *Modern Canonical Quantum General Relativity*; Cambridge Monographs on Mathematical Physics; Cambridge University Press: Cambridge, UK, 2007.
8. Bojowald, M. *Canonical Gravity and Applications: Cosmology, Black Holes, and Quantum Gravity*; Cambridge University Press: Cambridge, UK, 2010.
9. Gambini, R.; Pullin, J. *A First Course in Loop Quantum Gravity*; Oxford University Press: Oxford, UK, 2011.
10. Rovelli, C.; Vidotto, F. *Covariant Loop Quantum Gravity: An Elementary Introduction to Quantum Gravity and Spinfoam Theory*; Cambridge Monographs on Mathematical Physics; Cambridge University Press: Cambridge, UK, 2014.
11. Bojowald, M. Loop quantum cosmology. *Living Rev. Rel.* **2005**, *8*, 11. [CrossRef] [PubMed]
12. Ashtekar, A.; Singh, P. Loop Quantum Cosmology: A Status Report. *Class. Quant. Grav.* **2011**, *28*, 213001. [CrossRef]
13. Ashtekar, A.; Barrau, A. Loop quantum cosmology: From pre-inflationary dynamics to observations. *Class. Quant. Grav.* **2015**, *32*, 234001. [CrossRef]
14. Agullo, I.; Singh, P. Loop Quantum Cosmology. In *Loop Quantum Gravity: The First 30 Years*; Ashtekar, A., Pullin, J., Eds.; WSP: London, UK, 2017; pp. 183–240. [CrossRef]

15. Wilson-Ewing, E. Testing loop quantum cosmology. *Comptes Rendus Physique* **2017**, *18*, 207–225. [CrossRef]
16. Elizaga Navascués, B.; Marugán, G.A.M. Hybrid Loop Quantum Cosmology: An Overview. *Front. Astron. Space Sci.* **2021**, *8*, 81. [CrossRef]
17. Ashtekar, A.; Bianchi, E. A short review of loop quantum gravity. *Rept. Prog. Phys.* **2021**, *84*, 042001. [CrossRef]
18. Li, B.F.; Singh, P. Loop Quantum Cosmology: Physics of Singularity Resolution and its Implications. In *Handbook of Quantum Gravity*; Springer Nature: Singapore, 2023.
19. Agulló, I.; Wang, A.; Wilson-Ewing, E. Loop quantum cosmology: Relation between theory and observations. In *Handbook of Quantum Gravity*; Springer Nature: Singapore, 2023.
20. Gasperini, M.; Veneziano, G. Pre-big-bang in string cosmology. *Astropart. Phys.* **1993**, *1*, 317–339. [CrossRef]
21. Gasperini, M.; Maggiore, M.; Veneziano, G. Towards a nonsingular pre-big bang cosmology. *Nucl. Phys. B* **1997**, *494*, 315–330. [CrossRef]
22. Gasperini, M.; Veneziano, G. The Pre-big bang scenario in string cosmology. *Phys. Rept.* **2003**, *373*, 1–212. [CrossRef]
23. Haro, J. Cosmological perturbations in teleparallel Loop Quantum Cosmology. *J. Cosmol. Astropart. Phys.* **2013**, *11*, 068; Erratum in *J. Cosmol. Astropart. Phys.* **2014**, *5*, E01. [CrossRef]
24. Alonso-Serrano, A.; Liška, M.; Vicente-Becceril, A. Friedmann equations and cosmic bounce in a modified cosmological scenario. *Phys. Lett. B* **2023**, *839*, 137827. [CrossRef]
25. Conzinu, P.; Fanizza, G.; Gasperini, M.; Pavone, E.; Tedesco, L.; Veneziano, G. From the string vacuum to FLRW or de Sitter via α' corrections. *J. Cosmol. Astropart. Phys.* **2023**, *12*, 019. [CrossRef]
26. Khoury, J.; Ovrut, B.A.; Steinhardt, P.J.; Turok, N. The Ekpyrotic universe: Colliding branes and the origin of the hot big bang. *Phys. Rev. D* **2001**, *64*, 123522. [CrossRef]
27. Brown, M.G.; Freese, K.; Kinney, W.H. The Phantom bounce: A New oscillating cosmology. *J. Cosmol. Astropart. Phys.* **2008**, *3*, 002. [CrossRef]
28. Battefeld, D.; Peter, P. A Critical Review of Classical Bouncing Cosmologies. *Phys. Rept.* **2015**, *571*, 1–66. [CrossRef]
29. Brandenberger, R.; Peter, P. Bouncing Cosmologies: Progress and Problems. *Found. Phys.* **2017**, *47*, 797–850. [CrossRef]
30. Ijjas, A.; Steinhardt, P.J. Bouncing Cosmology made simple. *Class. Quant. Grav.* **2018**, *35*, 135004. [CrossRef]
31. Chandran, S.M.; Shankaranarayanan, S. Distinguishing bounce and inflation via quantum signatures from cosmic microwave background. *arXiv* **2024**, arXiv:2405.08543.
32. Taveras, V. Corrections to the Friedmann Equations from LQG for a Universe with a Free Scalar Field. *Phys. Rev. D* **2008**, *78*, 064072. [CrossRef]
33. Singh, P. Glimpses of Space-Time Beyond the Singularities Using Supercomputers. *Comput. Sci. Eng.* **2018**, *20*, 26–38. [CrossRef]
34. Corichi, A.; Singh, P. Quantum bounce and cosmic recall. *Phys. Rev. Lett.* **2008**, *100*, 161302. [CrossRef]
35. Kamiński, W.; Kolanowski, M.; Lewandowski, J. Dressed metric predictions revisited. *Class. Quant. Grav.* **2020**, *37*, 095001. [CrossRef]
36. Beetle, C.; Engle, J.S.; Hogan, M.E.; Mendonça, P. Diffeomorphism invariant cosmological sector in loop quantum gravity. *Class. Quant. Grav.* **2017**, *34*, 225009. [CrossRef]
37. Bojowald, M. Space–Time Physics in Background-Independent Theories of Quantum Gravity. *Universe* **2021**, *7*, 251. [CrossRef]
38. Li, B.F.; Singh, P.; Wang, A. Phenomenological implications of modified loop cosmologies: An overview. *Front. Astron. Space Sci.* **2021**, *8*, 701417. [CrossRef]
39. Yang, J.; Ding, Y.; Ma, Y. Alternative quantization of the Hamiltonian in loop quantum cosmology II: Including the Lorentz term. *Phys. Lett. B* **2009**, *682*, 1–7. [CrossRef]
40. Thiemann, T. Quantum spin dynamics (qsd). 2. *Class. Quant. Grav.* **1998**, *15*, 875–905. [CrossRef]
41. Thiemann, T. Quantum spin dynamics (QSD). *Class. Quant. Grav.* **1998**, *15*, 839–873. [CrossRef]
42. Assanioussi, M.; Dapor, A.; Liegener, K.; Pawłowski, T. Emergent de Sitter Epoch of the Quantum Cosmos from Loop Quantum Cosmology. *Phys. Rev. Lett.* **2018**, *121*, 081303. [CrossRef] [PubMed]
43. Assanioussi, M.; Dapor, A.; Liegener, K.; Pawłowski, T. Emergent de Sitter epoch of the Loop Quantum Cosmos: A detailed analysis. *Phys. Rev. D* **2019**, *100*, 084003. [CrossRef]
44. Li, B.F.; Singh, P.; Wang, A. Towards Cosmological Dynamics from Loop Quantum Gravity. *Phys. Rev. D* **2018**, *97*, 084029. [CrossRef]
45. Li, B.F.; Singh, P.; Wang, A. Qualitative dynamics and inflationary attractors in loop cosmology. *Phys. Rev. D* **2018**, *98*, 066016. [CrossRef]
46. Li, B.F.; Singh, P.; Wang, A. Genericness of pre-inflationary dynamics and probability of the desired slow-roll inflation in modified loop quantum cosmologies. *Phys. Rev. D* **2019**, *100*, 063513. [CrossRef]
47. Dapor, A.; Liegener, K. Cosmological Effective Hamiltonian from full Loop Quantum Gravity Dynamics. *Phys. Lett. B* **2018**, *785*, 506–510. [CrossRef]
48. Dapor, A.; Liegener, K. Cosmological coherent state expectation values in loop quantum gravity I. Isotropic kinematics. *Class. Quant. Grav.* **2018**, *35*, 135011. [CrossRef]
49. Han, M.; Liu, H. Loop quantum gravity on dynamical lattice and improved cosmological effective dynamics with inflaton. *Phys. Rev. D* **2021**, *104*, 024011. [CrossRef]

50. de Haro, J. The Dapor–Liegener model of loop quantum cosmology: A dynamical analysis. *Eur. Phys. J. C* **2018**, *78*, 926. [CrossRef]
51. Saini, S.; Singh, P. Generic absence of strong singularities and geodesic completeness in modified loop quantum cosmologies. *Class. Quant. Grav.* **2019**, *36*, 105014. [CrossRef]
52. Saini, S.; Singh, P. Von Neumann stability of modified loop quantum cosmologies. *Class. Quant. Grav.* **2019**, *36*, 105010. [CrossRef]
53. Li, B.F.; Singh, P. Loop quantum gravity effects might restrict a cyclic evolution. *Phys. Rev. D* **2022**, *105*, 046013.
54. Bonga, B.; Gupt, B. Phenomenological investigation of a quantum gravity extension of inflation with the Starobinsky potential. *Phys. Rev. D* **2016**, *93*, 063513. [CrossRef]
55. Zhu, T.; Wang, A.; Kirsten, K.; Cleaver, G.; Sheng, Q. Universal features of quantum bounce in loop quantum cosmology. *Phys. Lett. B* **2017**, *773*, 196–202. [CrossRef]
56. Zhu, T.; Wang, A.; Cleaver, G.; Kirsten, K.; Sheng, Q. Pre-inflationary universe in loop quantum cosmology. *Phys. Rev. D* **2017**, *96*, 083520. [CrossRef]
57. Shahalam, M.; Sharma, M.; Wu, Q.; Wang, A. Preinflationary dynamics in loop quantum cosmology: Power-law potentials. *Phys. Rev. D* **2017**, *96*, 123533. [CrossRef]
58. Shahalam, M.; Sami, M.; Wang, A. Preinflationary dynamics of $\alpha-$attractor in loop quantum cosmology. *Phys. Rev. D* **2018**, *98*, 043524. [CrossRef]
59. Sharma, M.; Shahalam, M.; Wu, Q.; Wang, A. Preinflationary dynamics in loop quantum cosmology: Monodromy Potential. *J. Cosmol. Astropart. Phys.* **2018**, *11*, 003. [CrossRef]
60. Sharma, M.; Zhu, T.; Wang, A. Background dynamics of pre-inflationary scenario in Brans-Dicke loop quantum cosmology. *Commun. Theor. Phys.* **2019**, *71*, 1205–1218. [CrossRef]
61. Shahalam, M.; Al Ajmi, M.; Myrzakulov, R.; Wang, A. Revisiting pre-inflationary Universe of family of α-attractor in loop quantum cosmology. *Class. Quant. Grav.* **2020**, *37*, 195026. [CrossRef]
62. Zhu, T.; Wang, A.; Kirsten, K.; Cleaver, G.; Sheng, Q. High-order Primordial Perturbations with Quantum Gravitational Effects. *Phys. Rev. D* **2016**, *93*, 123525. [CrossRef]
63. Levy, G.L.L.W.; Ramos, R.O. α-attractor potentials in loop quantum cosmology. *arXiv* **2024**, arXiv:2404.10149.
64. Li, B.F.; Singh, P.; Wang, A. Primordial power spectrum from the dressed metric approach in loop cosmologies. *Phys. Rev. D* **2020**, *101*, 086004. [CrossRef]
65. Li, B.F.; Olmedo, J.; Singh, P.; Wang, A. Primordial scalar power spectrum from the hybrid approach in loop cosmologies. *Phys. Rev. D* **2020**, *102*, 126025. [CrossRef]
66. Li, B.F.; Motaharfar, M.; Singh, P. Constraining regularization ambiguities in Loop Quantum Cosmology via CMB. *Phys. Rev.* **2024**, *110*, 066005. [CrossRef]
67. Li, B.F.; Singh, P. Close relationship between the dressed metric and the hybrid approach to perturbations in effective loop quantum cosmology. *Phys. Rev. D* **2022**, *106*, 086015. [CrossRef]
68. Meissner, K.A. Black hole entropy in loop quantum gravity. *Class. Quant. Grav.* **2004**, *21*, 5245–5252. [CrossRef]
69. Rovelli, C.; Smolin, L. Discreteness of area and volume in quantum gravity. *Nucl. Phys. B* **1995**, *442*, 593–622; Erratum in *Nucl. Phys. B* **1995**, *456*, 753–754. [CrossRef]
70. Ashtekar, A.; Lewandowski, J. Quantum theory of geometry. 1: Area operators. *Class. Quant. Grav.* **1997**, *14*, A55–A82. [CrossRef]
71. Ashtekar, A.; Sloan, D. Probability of Inflation in Loop Quantum Cosmology. *Gen. Rel. Grav.* **2011**, *43*, 3619–3655. [CrossRef]
72. Ashtekar, A.; Sloan, D. Loop quantum cosmology and slow roll inflation. *Phys. Lett. B* **2011**, *694*, 108–112. [CrossRef]
73. Kallosh, R.; Linde, A. Polynomial α-attractors. *J. Cosmol. Astropart. Phys.* **2022**, *4*, 017. [CrossRef]
74. Li, B.F.; Zhu, T.; Wang, A.; Kirsten, K.; Cleaver, G.; Sheng, Q. Preinflationary perturbations from the closed algebra approach in loop quantum cosmology. *Phys. Rev. D* **2019**, *99*, 103536. [CrossRef]
75. Baumann, D. Inflation. In *Proceedings of the Theoretical Advanced Study Institute in Elementary Particle Physics: Physics of the Large and the Small*; World Scientific: Singapore, 2011; pp. 523–686. [CrossRef]
76. Linde, A.D. Chaotic Inflation. *Phys. Lett. B* **1983**, *129*, 177–181. [CrossRef]
77. Starobinskii, A. Spectrum of relict gravitational radiation and the early state of the universe. *JETP Lett.* **1979**, *30*, 682–685.
78. Maeda, K.i. Inflation as a transient attractor in R^2 cosmology. *Phys. Rev. D* **1988**, *37*, 858–862. [CrossRef]
79. Ferrara, S.; Kallosh, R.; Linde, A.; Porrati, M. Minimal Supergravity Models of Inflation. *Phys. Rev. D* **2013**, *88*, 085038. [CrossRef]
80. Bhattacharya, S.; Dutta, K.; Gangopadhyay, M.R.; Maharana, A. α-attractor inflation: Models and predictions. *Phys. Rev. D* **2023**, *107*, 103530. [CrossRef]
81. Kallosh, R.; Linde, A.; Roest, D. Superconformal Inflationary α-Attractors. *J. High Energy Phys.* **2013**, *11*, 198. [CrossRef]
82. Adams, F.C.; Bond, J.R.; Freese, K.; Frieman, J.A.; Olinto, A.V. Natural inflation: Particle physics models, power law spectra for large scale structure, and constraints from COBE. *Phys. Rev. D* **1993**, *47*, 426–455. [CrossRef] [PubMed]